Università degli studi di Padova
Department of Information Engineering

Master Thesis in

TELECOMMUNICATION ENGINEERING

Simulation analysis of algorithms for interference management in 5G cellular networks using spatial spectrum sharing

Supervisor
Dr. Michele Zorzi

Candidate
Mattia Rebato

Academic Year 2014/2015

A tutti coloro che mi hanno sostenuto in questo lungo percorso...

Abstract

With the increasing demand of data and the growth of the connections between devices, a new generation of mobile networks, denominated 5G, is necessary in order to reach data rates required.

In this thesis project we completely overhaul past techniques to the new millimeter wave frequencies used in 5G and the aim is to study algorithm, protocols and architectures enablers to allow spatial spectrum sharing between different networks at these frequencies.

With the use of specific modules of the network simulator ns-3, studies of simulations has been made in order to analyse performance of several sharing procedure with the goal of increase performance in a mobile network of fifth generation. The simulated scenarios will be deeply examined though figures and graphs which will be used to compare all the procedures' performances.

Sommario

Con l'aumentare del traffico dati e la crescita delle connessioni tra dispositivi, un nuovo standard per reti cellulari, chiamato 5G, è necessario in modo da soddisfare i flussi dati richiesti.

In questo progetto di tesi abbiamo completamente revisionato i precedenti protocolli LTE, in modo da poterli usare su frequenze con onde millimetriche usate nel 5G, lo scopo è quello di studiare algoritmi, protocolli e architetture in grado di realizzare una condivisine spaziale dello spettro tra diversi networks.

Utilizzando specifici moduli del simulatore di reti ns-3, abbiamo realizzato e studiato simulazioni in modo da analizzare il comportamento di alcune tecniche per la condivisione di risorse, con l'obiettivo di aumentare le prestazioni in una rete cellulare di quinta generazione. Gli scenari simulati saranno esaminati a fondo con l'uso di figure e grafici in modo da confrontare le prestazioni delle varie procedure.

Contents

List of Figures

List of Tables

Acronyms

μW	micro Wave
AMC	Adaptive Modulation and Coding
AoA	Angle of Arrival
AoD	Angle of Departures
AP	Access Point
BER	Bit Error Rate
BF	Beamforming
BS	Base Station
CCU	Central Coordination Unit
CC	Coordination Context
CQI	Channel Quality Indicator
CU	Coordination Unit
DL	Downlink
IoT	Internet of Things
IT	Interference Threshold
LoS	Line of Sight
LSA	Licensed Shared Access
LTE	Long Term Evolution
MCS	Modulation and Coding Scheme

MIMO	Multiple Input and Multiple Output
mmW	millimeter Wave
NGMN	Next Generation Mobile Networks
NLoS	Non Line of Sight
ns-3	networks simulator 3
NYU	New York University
OFDMA	Orthogonal Frequency-Division Multiple Access
OFDM	Orthogonal Frequency Division Multiplexing
PHY	Physical
RB	Resource Block
RF	Radio Frequency
RNTI	Radio Network Temporary Identifier
RR	Round Robin
SAP	Service Access Point
SINR	Signal to Interference plus Noise Ratio
SPSH	Spectrum Sharing
TB	Transport Block
TDD	Time Division Duplex
TDMA	Time Division Multiple Access
TU	Training Unit
UE	User Equipment
ULA	Uniform Linear Array
UL	Uplink
WLAN	Wireless Local Area Networks

Chapter 1

Introduction

With the increasing demand of data and the growth of the connection among devices, a new generation of mobile networks is necessary in order to reach the challenges required. For this reason, the Next Generation Mobile Networks (NGMN) alliance and other leadering companies affirm that, for 5G, data rates of several tens of Mb/s should be supported for tens of thousands of users, several hundreds of thousands of simultaneous connections should be supported for massive sensor deployments, latency significantly reduced to 1 ms end-to-end and 1 Gbit/s should be offered, simultaneously, to tens of workers on the same office floor [1], [2], [7].

In Figure 1.1 are shown the challenges required in the 5G standard compared with the actual 4G Long Term Evolution (LTE). Several studies are necessary in order to reach the challenges required for the future generation of mobile communications.

In addition to simply providing faster speed, NGMN predicts that 5G networks will also need to meet the needs of new use-cases such as the Internet of Things (IoT) as well as broadcast-like services and lifeline communications in times of natural disaster.

These demands for very high system capacity and very high end-user data rates can be met by networks with distances between access nodes ranging from a few meters in indoor deployments up to roughly 200 m in outdoor deployments, consequently with an infra-structure density considerably higher

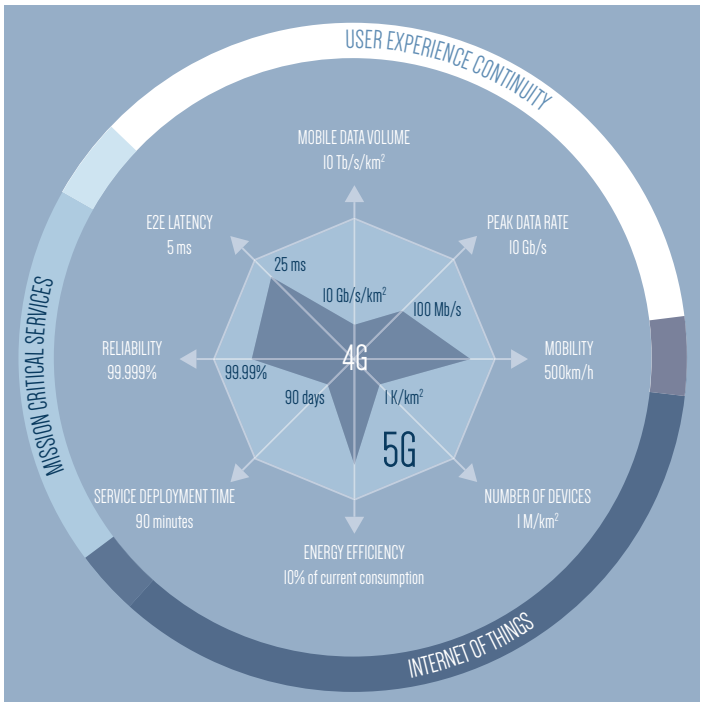

Fig. 1.1: Comparison specifics of standards 4G and 5G. Figure from [1].

than the most dense networks of today [5], [8].

The first issue to address in order to achieve the challenges of the standards is the identification of the frequencies to use. Given that the current micro-wave (μW) spectrum under 5 GHz is very fragmented and crowded, new frequencies are necessary to achieve the high throughput required and a possible solution to the problem is the use of millimeter Wave (mmW) communications. mmW frequencies, from 30 GHz to 300 GHz[1], has been identified as one of the most promising techniques in the future of wireless communications and for the 5th generation of cellular technology [9], [10], [11].

In a different way from the current frequencies used for mobile communication, a lot of attenuation problems are present in mmW, due to the high frequencies used. These attenuation problems can be alleviate implementing techniques such as massive multiple-input and multiple-output (MIMO) and beamforming (BF).

[1]While the mmW spectrum is defined as the band between 30-300 GHz, industry has loosely considered mmW to be any frequency above 10 GHz.

The potential for system bandwidths much greater that what is available in the traditional cellular bands (around 100 times greater) together with the potential for large scale antenna arrays (due to shorter wavelengths which permit to deploy a great amount of antenna elements in the same area) make these bands attractive for high-capacity small-cell deployment for dense use scenarios [12].

Compared to traditional cellular systems operating around 2 GHz, utilizing new bands means facing new challenges, especially in terms of less favourable link budgets due to higher path loss (since now we are working at higher frequencies) and higher shadowing losses (since millimeter waves are more sensitive to diffraction and dispersion effects), which result in many radio propagation issues, that we have to deal with. All these problems make us understand the importance of defining new standards, protocols and algorithms, with respect to those already existing for the current 4G-LTE cellular systems, in order to deal with the upcoming mmW networks.

In this thesis project we completely overhaul past techniques to the new frequencies and the aim is to study algorithms, protocols and architectures able to allow spatial spectrum sharing between different networks at mmW frequencies.

Some possible solutions already used for 4G-LTE, like the ones in [13] and [14] where a trade-off for Spectrum Sharing (SPSH) is done, can be implemented also for mmW but particular studies are needed due to the large attenuation present at the high frequencies. Starting with that, we design and analyse possible algorithms which perform a spatial spectrum sharing that aims at increasing throughput by coordinating transmission in the spatial-time-frequency domain.

In order to study possible solutions we simulate the protocols in the discrete networks simulator ns-3 [15], in particular we use specific ns-3 modules created for the simulation of a mmW environment [16].

The rest of the thesis is organized as follows: Chapter 2 presents a global overview of the 5G standard and millimeter waves then Chapter 3 introduces the concept of sharing of resources. Chapter 4 presents the ns-3 simulator

describing the structure in modules and how it works, after that Chapter 5 describes the protocols studied and introduced in this thesis. Then Chapter 6 report a description of the scenarios implemented and result of simulation. Conclusion and future works are provided in Chapter 7.

Chapter 2

Millimeter waves in 5G cellular systems

2.1 5G overview

5G is the next step in the evolution of mobile communication, research is just at the beginning therefore there isn't a unique definition for 5G yet. It will be a key component of the Networked Society[1] and will help realize the vision of essentially unlimited access to information and sharing of data anywhere and anytime for anyone and anything [2].

5G will therefore not only be about mobile connectivity for people. Rather, the aim of 5G is to provide ubiquitous connectivity for any kind of device and any kind of application that may benefit from being connected.

Mobile broadband will continue to be important and will drive the need for higher system capacity and higher data rates. This new generation will also provide wireless connectivity for a wide range of new applications and use cases, including wearables, smart homes, traffic safety control, and critical infrastructure and industry applications, as well as for very-high-speed media delivery.

In contrast to earlier generations, 5G wireless access should not be seen

[1]The Networked Society is a term used to describe a future ecosystem, envisioned by the Information and Communications Technology (ICT) company Ericsson, in which widespread internet connectivity drives change for individuals and communities.

as a specific radio-access technology. Rather, it is an overall wireless-access solution addressing the demands and requirements of mobile communication beyond 2020. LTE will continue to develop in a backwards-compatible way and will be an important part of the 5G wireless-access solution for frequency bands below 6 GHz [2]. Figure 2.1 shows a possible overall 5G wireless-access solution consisting of LTE evolution and new technology working at mmW frequencies (above 6 GHz).

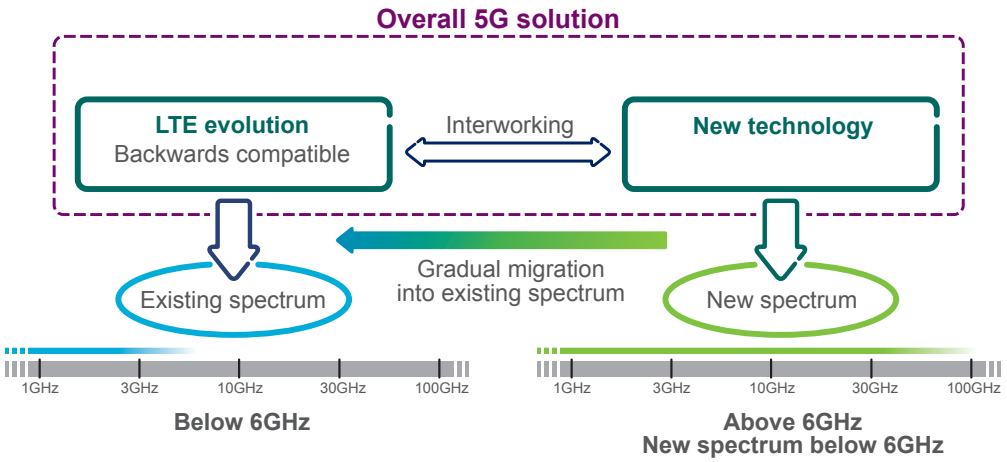

Fig. 2.1: Overall 5G wireless-access solution consisting of LTE evolution and new technologies. Figure from [2].

Due to the spectrum scarcity in microwave bands used by legacy communication technologies, mmW bands are considered as a promising enabler for 5G cellular networks to provide multi-gigabit wireless access. The available spectrum at these higher frequencies can be easily 200 times greater than all cellular allocations today.

2.2 Millimeter waves (mmW)

Although mmW frequencies can be used, mmW communications exhibit high attenuation, vulnerability to obstacles and sparse-scattering environments, which are not taken into account in the existing cellular wireless design approaches.

In a different way, the small wavelengths of mmW signals make it possible to incorporate a large number of antenna elements both at the Base Station (BS) and at the User Equipment (UE), which in turn lead to high directivity gains and fully-directional communications. This level of directionality can result in a network that is noise-limited as opposed to interference-limited.

The significant differences between mmW networks and traditional ones challenge the classical design constraints, objectives, and available degrees of freedom. An example of this can be a scenario of Non Line of Sight (NLoS), where communication between transmitter and receiver can not be achieved due to the high attenuations [8]. This demands a reconsideration of almost all design aspects in mmW systems.

2.2.1 Challenges of mmW

Despite the potential of mmW cellular systems, there are a number of key challenges to realize the vision of cellular networks in these bands [17]:

- **Range and directional communication**: Friis' transmission law, in the equation below,

$$P_r = P_t G_t G_r \left(\frac{\lambda}{4\pi R}\right)^2 \tag{2.1}$$

  states that the free space omnidirectional path loss grows with the square of the frequency. In the equation: P_r and P_t are respectively the power received and the power transmitted, G_t and G_r are the gains of the tx and rx antennas, R is the distance between the receiver and transmitter and λ is the wavelength. However, the smaller wavelength of mmW signals also enables proportionally greater antenna gain (knowing that the gain is given by: $G = \frac{4\pi}{\lambda^2} A_{eff}$) for the same physical antenna size. Consequently, the higher frequencies of mmW signals do not in themselves result in any increased free space propagation loss, provided the antenna area remains fixed and suitable directional transmissions are used. This is also confirmed from measurements in [17].

- **Atmospheric gaseous losses**: This kind of attenuation is typically less than a few dB per kilometer (as Figure 2.2 shows) excluding particular absorption bands like the ones of oxygen (near 60 GHz) and water vapor (near 20 and 200 GHz). In the particular case of small cells/areas, some hundreds of meters, this attenuation is not so relevant.

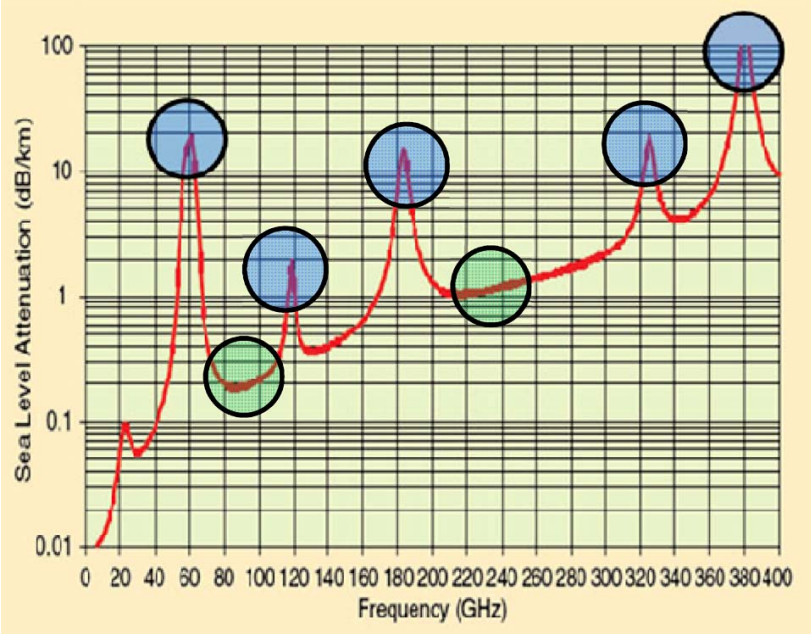

Fig. 2.2: Atmospheric absorption across mmW bands. Figure from [3].

- **Shadowing**: A more significant concern for range is that mmW signals are extremely susceptible to shadowing. For example, materials such as brick can attenuate signals by as much as 40 to 80 dB and the human body itself can result in a 20 to 35 dB loss. On the other hand, humidity and rain fades (common problems for long range mmW backhaul links) are not an issue in cellular systems. Figure 2.3 shows that even in a very heavy rainfall, rain fades are typically less than a dB per 100 m meaning they will have minimal impact in cellular systems with cell radii smaller than 200 m. Also, the human body and many outdoor materials are very reflective, and therefore are important scatterers for mmW propagation.

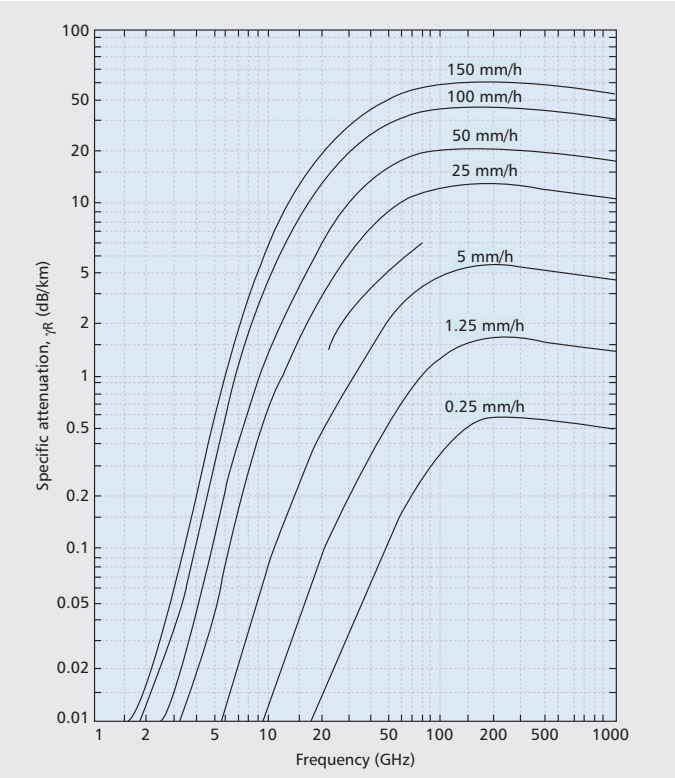

Fig. 2.3: Rain attenuation in dB/Km at various rainfall rates. Figure from [4].

- **Rapid channel fluctuations and intermittent connectivity**: For a given mobile velocity, channel coherence time is linear in the carrier frequency, meaning that it will be very small in the mmW range. In addition, high levels of shadowing imply that the appearance of obstacles will lead to much more dramatic swings in path loss, although beam-steering may overcome this. Also, mmW systems will be inherently built of small cells, meaning that relative path losses and cell association also change rapidly. From a system perspective, this implies that connectivity will be highly intermittent and communication will need to be rapidly adaptable.

In conclusion, after excluding some sub-bands with severe atmospheric absorption and assuming 40% of the remaining spectrum potentially becomes available over time, a possible 100 GHz new spectrum among the mmW band could be opened up for future mobile communication use [9], [17].

2.2.2 Benefits of mmW

Despite all the challenges listed above, the use of mmW also provides some advantages.

Due to the small wavelength, the use of MIMO is easily implementable and this is already a key technology in supporting high data rates in 4G systems. MIMO enables multi-stream transmission for high spectrum efficiency, improved link quality and adaptation of radiation patterns for signal gain and interference mitigation via adaptive beamforming using antenna arrays [18], [19].

Since the tiny wavelengths allow for dozens to hundreds of antenna elements to be placed in an array on a relatively small physical platform at the BS, or access point, massive MIMO can be used. Extra antennas help by focusing energy into ever smaller regions of space to bring huge improvements in throughput and radiated energy efficiency. Other benefits of massive MIMO include extensive use of inexpensive low-power components, reduced latency, simplification of the MAC layer, and robustness against intentional jamming [19], [20].

All these aspects are perfect for scenarios of mmW communications. In addition, MIMO systems allow to use BeamForming (BF) and so obtain a directional signal transmission or reception. This is achieved by combining elements in a phased array in such a way that signals at particular angles experience constructive interference while others experience destructive interference. BF can be used at both the transmitting and receiving ends in order to achieve spatial selectivity [21].

After the list of pros and cons, all the studies and in-the-field simulations have identified mmW frequencies as the means to carry communication in the systems of fifth generation.

Chapter 3

Spatial Spectrum Sharing

The term Spectrum Sharing (SPSH) is used to indicate the sharing of spectrum among multiple operators or devices in a wireless environment. The main concept behind this technique is to share unused spectrum of a network with others that need more resources at particular time. An example of SPSH can be seen in Figure 3.1.

Spectrum sharing may be *orthogonal*, meaning that access to the shared resources by either operator automatically excludes the other one, or *non-orthogonal*, where the operators are allowed to use the same transmission frequency resource simultaneously.

Adding the word *spatial*, we indicate a sharing of resources that is not only in the frequency domain but also in the spatial domain: computing transmission in directions that do not interfere.

In such a way, spatial SPSH coordinates transmission schemes and increases the performance and use of resources.

3.1 Spectrum Sharing in 4G-LTE

In 4G-LTE, several techniques have been studied in order to improve the efficiency of the allocation. An important solution, taken as an example for this project, is the one proposed in [13].

Spectrum allocation policies, which impose exclusive usage to a licensed

operator, may lead to inefficient management and waste of resources. The use of the same frequency band by multiple operators, that SPSH is supposed to realise, helps to improve the efficiency of the spectrum allocation and therefore the performance of the networks involved.

Consider a scenario where two mobile operators managing neighboring cells are serving two groups of users in the same geographical region. The operators have the opportunity to share, partially or totally, their available spectrum, as shown in Figure 3.1.

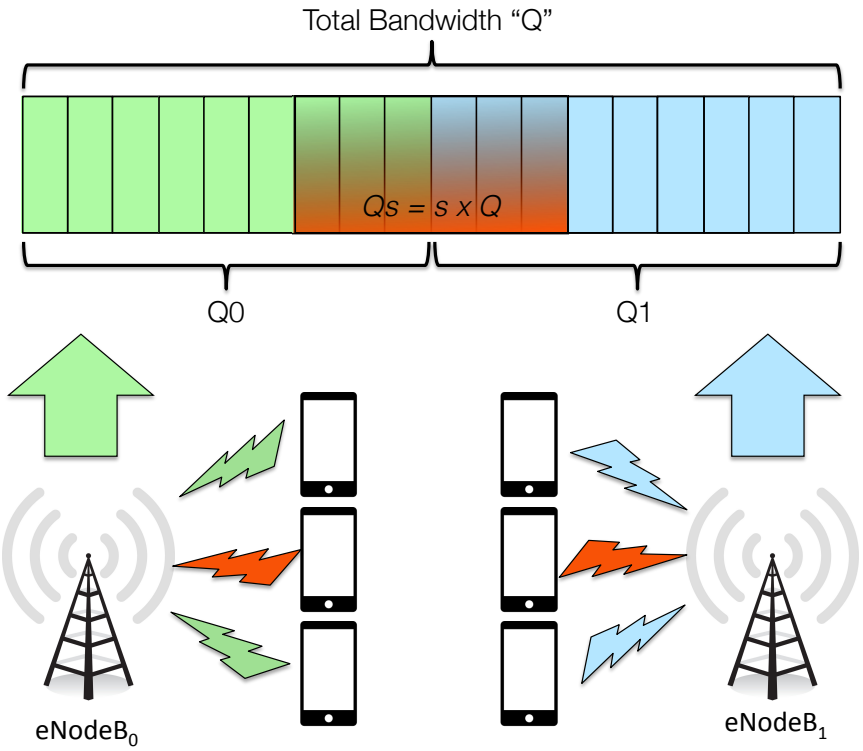

Fig. 3.1: Example scenario of Spectrum Sharing.

The spectrum is divided into groups of adjacent sub-carriers, called sub-channels; a private subchannel can be accessed by a single user whereas a shared one can be accessed by one user per operator, depending on the scheduling algorithm used. Moreover, orthogonal sharing is necessary in a way not to introduce problems of inter-operator interference.

Results of simulations, provided in [13] and [14], are expressed in terms

of throughput, which represents the average sum data rates delivered to all the UEs. The results show that the throughput increases a lot in the case of perfect orthogonality. Improvements can be obtain also in a non-orthogonal scenario. Moreover, [13] shows that it is always better to have a full sharing of the available frequencies. This may not be possible due to internal policy requirements of the operators; nevertheless, the larger the fraction of shared spectrum, the better. For the simulations, a particular extension of ns-3 design has been used in [22].

3.2 Spatial SPSH in 5G

3.2.1 State of the art

In order to face the increase of data demand, a new technology able to support high amounts of traffic is required. To do so, some researcher have started to investigate this field and innovative solutions have been proposed. However, the new generation of mobile networks needs more and more resources to guarantee the high quality required by the end users. To address this issue, focusing on SPSH, some papers provide sharing techniques between different networks. Since mmW is a new technology, there is a lot of study to do and not a lot of work has been done so far. In fact, most of the prior art refers to SPSH in Wireless Local Area Networks (WLAN) instead of cellular networks.

In [23] a mechanism for allowing two different 802.11ad[1] Access Points (AP) to transmit over the same time/frequency resources is proposed, effectively in a way to enable spectrum sharing. This is realised by introducing a new signalling report broadcast by each AP, to allow it to establish an interference database and based on these distributed databases a new inter-network MAC approach is proposed.

[1]IEEE 802.11ad is an amendment that defines a new physical layer for 802.11 networks to operate in the 60 GHz millimeter wave spectrum. Products implementing the 802.11ad standard are being brought to market under the WiGig brand name. The certification program is now being developed by the Wi-Fi Alliance instead of the now defunct WiGig Alliance. The peak transmission rate of 802.11ad is 7 Gbit/s.

Here an open issue is how the interference can be estimated by the different nodes with the current versions of the standard. Further analysis is also needed to understand if this MAC approach can be implemented in a fully distributed way.

A similar approach is proposed in [24], with both a centralised and a distributed architecture. In particular, [24] instead of being implemented for WLAN, is already designed for 5G mmW cellular networks. From a deployment assumption perspective, this document considers the case of two partially overlapping cellular networks, in which only a subset of the nodes is interfered. In the centralised case, a new architectural entity (referred as central coordination functionality) is connected to multiple mmW networks, receives the interference information measured by each network and makes the decision on which links cannot be scheduled at the same time. A centralised solution is expected to be useful for scenarios where a centralised entity is already present for other reasons. Centralised control is capable of providing optimal resource allocation for the entire network and exhibits a fast convergence, but the required amount of signaling may be excessive for medium to large-sized networks. In the decentralised case, the victim network sends a message to the interfering network with a proposed coordination pattern. By definition, distributed control does not require a central entity and allows BSs and UEs to make autonomous user association decision by themselves through the interaction between BSs and UEs. The two networks can further refine the coordination pattern via multiple stages.

Results in [24] provide that with the use of an interference database larger improvements can be obtained.

In [25] and [26], spectrum reuse mechanisms are proposed to coordinate multiple ad-hoc links belonging to the same AP. In particular [25] proposes an extension of the BF training mechanism in 802.11ad to incorporate interference measurements. Moreover, a centralised interference-aware scheduling is proposed. A similar centralised approach is proposed in [26], but is instead based on beam index information rather than interference measurements.

In [27] a multi-carrier waveform based inter-operator spectrum sharing concept is presented. The proposed concept is a strong extension of OFDMA-based schemes and can support coordinated inter-operator SPSH in various scenarios, including mutual renting (where operators mutually allow other operators to "rent" parts of their licensed resources), co-primary sharing, Licensed Shared Access (LSA), etc. The key element proposed is a two-stage spectrum allocation procedure where the first stage is an inter-operator spectrum allocation, then after that, the second stage is a short term pre-operator resource allocation to users.

According to this state of the art, in the next section we will analyse the limitations in order to solve issues and provide spatial SPSH between mobile operators of fifth generation. Moreover we will focus on the training procedure presented in [24], studying the result in a scenario where a dense urban channel model is applied and with a fully directional transmission.

3.2.2 Analysis and limitations

Due to high frequency bands and small coverage, mmW networks are predominantly expected to be deployed in the form of *coverage islands* serving high traffic density areas (e.g., an office building, a shopping mall, etc.). Different mmW networks, representing different operators, may be running in the same or overlapping area.

Protocols and procedures already implemented in 4G can still be used for 5G but some differences are present and new strategies should be added to the current implementation. The main new difference is that communications between BS and UEs will be perform in a directional way. Directional transmission is really different in comparison with omnidirectional, in fact frequency reuse and spectrum sharing can be inefficient in a scenario where directional transmission is implemented.

The use of directional transmission can be perfect to achieve high data rates. In a scenario in which nearest cells can use the same frequencies

(transmitting with large bandwidth) and perform mechanisms to avoid interference with directional transmission, high data rates for a large number of users can be provided. This is exactly what is required in a millimeter wave communication.

Therefore, for these reasons, this thesis studies a new approach of Spatial Spectrum Sharing that can be used in 5G system.

Chapter 4

ns-3 and mmW modules

4.1 Description

ns-3 is a discrete-event network simulator for Internet systems, targeted primarily for research and educational use. ns-3 is an open-source software, licensed under the GNU GPLv2 license, and is publicly available for research, development and use [15].

Due to the complexity of the networks this simulator helps to perform computations that are difficult to perform theoretically.

Another important characteristic of ns-3 is its modularity. In particular, the ns-3 software infrastructure encourages the development of simulation models which are sufficiently realistic to allow ns-3 to be used as a real-time network emulator, interconnected with the real world and which allows many existing real-world protocol implementations to be reused within ns-3.

For this project, we used a particular mmW module (described in Section 4.2) developed by a research group at New York University (NYU) Wireless [28] that helps to simulate mmW mobile networks scenarios [16].

All the simulations designed in this thesis are made with the version 23 of ns-3 (released in May 2015).

4.2 mmW modules

The research group at NYU has developed a fully customized model where the users can plug in various parameters in order to describe the behavior of the mmW channel and devices [16].

The aim of the framework is to enable researchers to flexibly use this module for various scenarios and compute simulations of mmW environments. Part of the design is made following specific recent real-world measurements at 28 and 73 GHz introduced by [5]. These measurements were made in New York City to derive detailed spatial statistical models of the channels and uses these models to provide a realistic assessment of mmW micro and pico cellular networks in a dense urban deployment.

The framework includes a basic implementation of mmW devices, which comprises the propagation and channel model, the physical (PHY) layer, and the MAC layer. The design of this module, developed in C++, is completely inspired by the ns-3 LENA module [29].

4.2.1 Physical layer (PHY): Frame and Transmission schemes

The PHY layer implemented in the modules is equipped with some features that can be set with particular values, which creates scenarios to simulate. Among all the features that the PHY layer provides, we focus on the ones used for our simulations that are: a fully customizable Time Division Duplex (TDD) frame structure, a radio characterization along with supporting MIMO techniques such as BF, a decoding error model at the receiver side and an interference model.

Frame structure

The TDD frame structure is organized as follows. Each frame is subdivided into a number of subframes of fixed length specified by the UE. Each subframe in turn is split into a number of slots of fixed duration. Each slot comprises a specific number of Orthogonal Frequency Division Multiplexing (OFDM)

symbols. A slot can be used for either control (c) or data (d), and assigned to either uplink (UL) or downlink (DL).

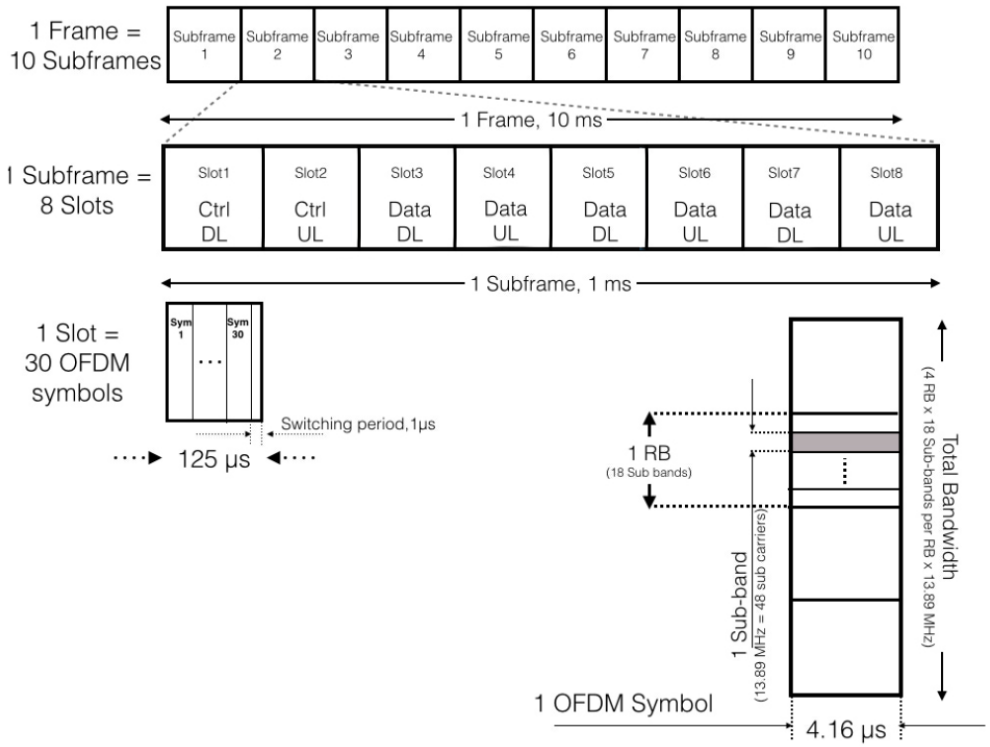

Fig. 4.1: Example of mmW frame structure.

In all simulations provided in this thesis, we use a frame structure as in Figure 4.1, where each frame of length 10 ms is split in time into 10 subframes, each of duration 1 ms. Each subframe is further divided into 8 slots where each slot is of length 125 μs, representing 30 OFDM symbols of length 4.16 μs. The first two slots are used for control and data in the DL and UL directions, respectively. Slots 3,5 and 7 are allocated for DL while slots 4,6 and 8 for UL data transmission. In particular, a switching gap of 1 μs is introduced each time the allocated direction changes from uplink to downlink or vice-versa.

In the frequency domain, the entire bandwidth of 1 GHz is divided into 4 Resource Blocks (RBs). Each RB is subdivided into 18 sub-bands, each of

Parameter	Default Value
Symbol per slot	30
Symbol length	4.16 μs
Slots per subframe	8
Subframe per frame	10
Number reference symbols	6
TDD pattern	ccddddddd
Subcarriers per subband	48
Subbands per RB	18
Subband width	13.89 MHz
Number RB	4
Center frequency	28 GHz

Table 4.1: Parameters for configuring the mmW frame structure.

width 13.89 MHz, making a total of 72 sub-bands for the entire bandwidth. Each of these sub-bands is composed of 48 sub-carriers.

Transmission schemes

The physical layer implemented in the modules handles the transmission and reception of signal, simulates the start and the end of frames, delivers data packets and control message received over the channel to the MAC layer and models the decoding error for the received signal and calculates the metrics, such as the Signal to Interference plus Noise Ratio (SINR).

Based on the total band of frequency available for transmission, the PHY computes the transmission power spectral density using the *mmWaveSpectrumValueHelper* component and uses this value for the signal transmission. When a UE receives a data packet, the PHY layer computes the SINR of the received signal taking into account the MIMO BF gain. The PHY layer at the user device maps the calculated SINR into a Channel Quality Indicator (CQI), which is fed back to the base station for the resource allocation.

Channel Quality Indicator (CQI) CQI is a measure of the quality of the signal provided by the UE to the BS. The BS obtains the CQI after

computing the spectral efficiency with the following equation:

$$\eta = \log_2 \left(1 + \frac{SINR}{\Gamma}\right) \tag{4.1}$$

then chooses the most suitable modulation and coding scheme for each UE using the Adaptive Modulation and Coding (AMC) module [30]. In (4.1), Γ is a coefficient introduced to model the difference between the theoretical bound and the performance of real modulation and coding scheme; such a coefficient depends on the Bit Error Rate (BER): $\Gamma = -\ln(5 \cdot BER)/1.5$. For the computation of the SINR we refer to the section about interference in the following pages.

The procedure of mapping each CQI value in a Transport Block (TB) size permits to compute the most suitable modulation and coding scheme for the communication link. The higher the CQI, the higher the size of the TB allocated.

4.2.2 Physical layer (PHY): Channel model

With regard to the channel model, it is important to highlight that, in a mmW channel, the use of a multi-antenna approach is implemented to perform BF, in order to increase the gain, which is particularly critical in millimeter wave communication. This gain can be much more exploited, with respect to the classical cellular networks. A large number of antenna elements can be packed into a small form factor in mmW bands due to the much smaller wavelength than legacy cellular bands. Then MIMO becomes more feasible and can be also useful for transmitting signals over a long distance in the environments [31].

As illustrated in Figure 4.2, the models take into account a large number of procedures to capture the main characteristics of the mmW propagation. The key contribution here, as already mentioned, relates to the computation of the multi-antenna gains, which is particularly critical for mmW communications.

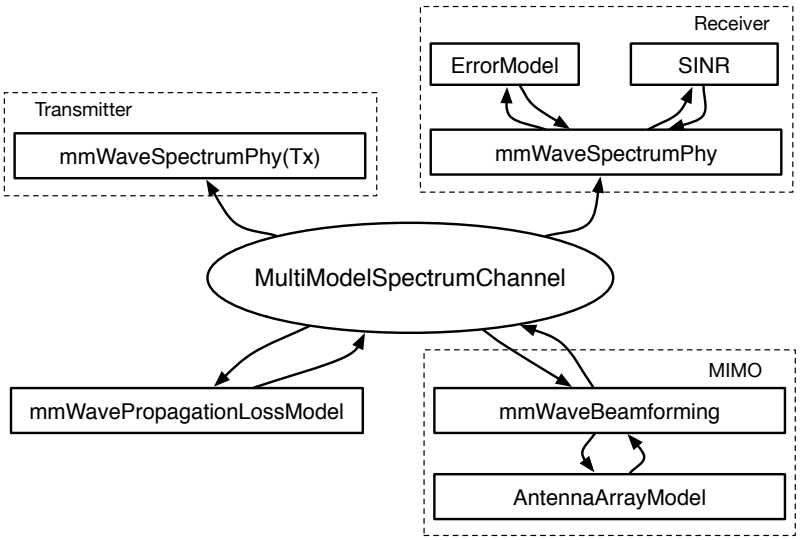

Fig. 4.2: Procedure to capture characteristic of the mmW channel model.

The link budget for the mmW propagation channel is given by:

$$P_{RX} = P_{TX} + G_{BF} - PL - SW \tag{4.2}$$

where P_{RX} is the total received power expressed in dBm, P_{TX} is the transmit power, G_{BF} is the gain obtained using BF technique, then PL and SW represent the pathloss and shadowing, respectively.

The mmW modules can work in three different states of pathloss model, depending on the scenario we are working on. These possible states are: Line of Sight (LoS), Non-Line of Sight (NLoS) and outage.

For every link, the code determines the channel state through the following procedure. Based on the distance between the two nodes of the link (transmitter and receiver), the probability of being in one of the states (p_{LoS}, p_{NLoS}, p_{out}) is computed then picking a random number in the interval $[0, 1]$ and comparing it with the probability associated to each channel state. In particular, if $p_{ref} < p_{LoS}$, the channel will be in a LoS configuration, else if $p_{LoS} < p_{ref} < (p_{LoS} + p_{NLoS})$ the configuration will be NLoS. Otherwise, it will be outage. For mmW systems, [5] proposes to add an additional state,

so that each link can be in one of three conditions: LoS, NLoS or outage. In the outage condition, is assumed that there is no link between the TX and RX.

By adding this third state with a random probability for a complete loss, the model provides a better reflection of outage possibilities inherent in mmW. As a statistical model, the probability functions above for the three states are of the form:

$$\begin{aligned} p_{out}(d) &= \max(0, 1 - e^{-a_{out}d + b_{out}}) \\ p_{LoS}(d) &= (1 - p_{out}(d))e^{-a_{los}d} \\ p_{NLoS}(d) &= 1 - p_{LoS}(d) - p_{out}(d) \end{aligned} \tag{4.3}$$

where the parameters a_{los}, a_{out} and b_{out} are parameters that are fit from the data [5]. Figure 4.3 shows the fractions of point that were observed to be in each of the three states - outage, NLoS[1] and LoS.

For each link, on determining the channel state, the pathloss and shadowing are obtained by:

$$PL(d)[dB] = \alpha + \beta 10 \log_{10}(d) + \xi \tag{4.4}$$

where $\xi \sim N(0, \sigma^2)$ represents the shadowing, d is the distance between receiver and transmitter, while the value of the parameters α, β and σ are given by [5], for each scenario:

	28 **GHz**			73 **GHz**		
	α	β	σ [dB]	α	β	σ [dB]
NLoS	72	2.92	8.7	86.6	2.45	8
LoS	61.4	2	5.8	69.8	2	5.8

Table 4.2: Parameters α, β and σ in the case of NLoS or LoS for the two frequencies: 28 and 73 GHz.

The parameters provided by [5] have been computed only for the two frequencies of 28 and 73 GHz, which are thus the only two usable in the

[1]In a dense urban environment, where measurements had been conducted, signals can be severely vulnerable to shadowing resulting in outages, rapidly varying channel conditions and intermittent connectivity. This issue is of particular concern in cluttered, urban deployments where coverage frequently requires NLoS links.

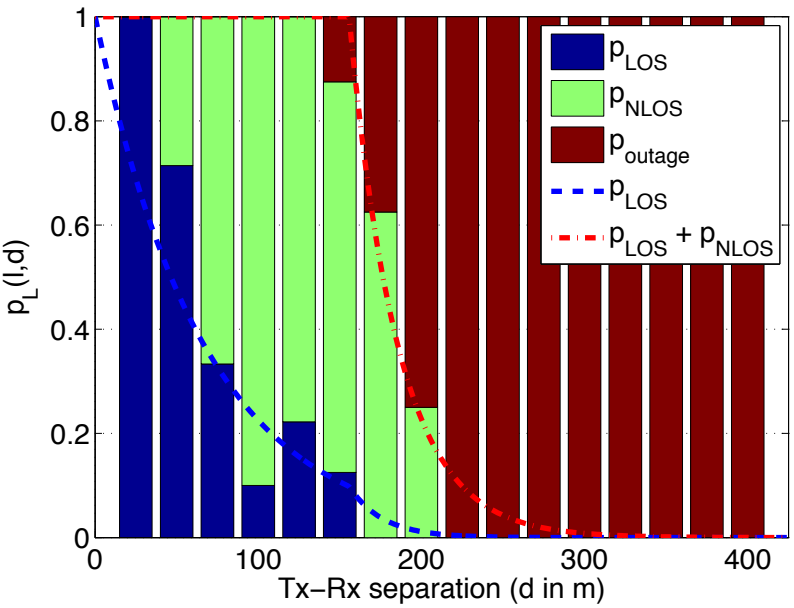

Fig. 4.3: The fitted curves and the empirical values of $p_{LoS}(d)$, $p_{NLoS}(d)$ and $p_{out}(d)$ as a function of the distance d. Measurement data is based on 42 TX-RX location pairs with distances from 30 m to 420 m at 28 GHz. Figure from [5].

simulations; more evaluation will be necessary in order to have information about the losses for all the possible mmW frequencies.

MIMO

The code models the mmW channel, following the Winner II model [6], as a combination of $N \sim \max\{Poisson(\lambda), 1\}$ clusters[2], each composed of several subpaths L_k, as in Figure 4.4.

The number N of *path-clusters* is described by a fraction of the total power and central azimuth (horizontal) and elevation (vertical) Angles of Arrival (AoA) and Angle of Departures (AoD), which are respectively θ_{kl}^{rx}, ϕ_{kl}^{rx}, θ_{kl}^{tx}, ϕ_{kl}^{tx}.

[2] After many experiments conducted in [5], it has been set $\lambda = 1.8$ for the 28 GHz band and $\lambda = 1.9$ for the 73 GHz band.

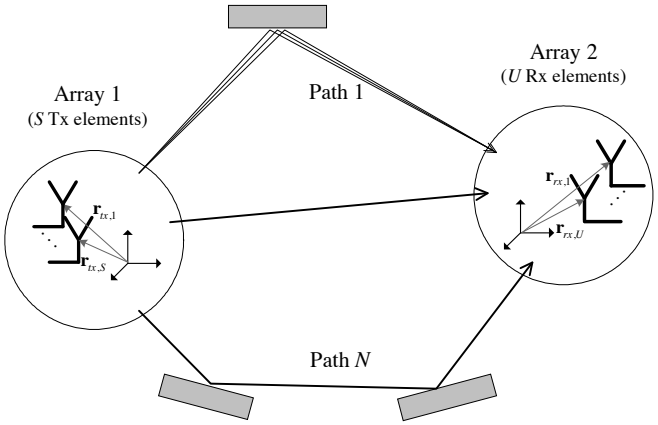

Fig. 4.4: Cluster configuration of the channel. Figure from [6]

Thus, the channel matrix is described as follows:

$$H(t,f) = \frac{1}{\sqrt{L}} \sum_{k=1}^{N} \sum_{l=1}^{L_k} g_{kl}(t,f) \mathbf{u}_{rx}(\theta_{kl}^{rx}, \phi_{kl}^{rx}) \mathbf{u}_{tx}^{*}(\theta_{kl}^{tx}, \phi_{kl}^{tx}) \tag{4.5}$$

where $g_{kl}(t,f)$ refers to the small-scale fading over time and frequency on the l-th subpath of the k-th cluster and $\mathbf{u}_{rx}(\cdot)$, $\mathbf{u}_{tx}(\cdot)$ are the vector response functions for the receiver and transmitter antenna arrays to the AoA and AoD.

The small-scale fading is generated based on the number of clusters, number of subpaths per cluster, Doppler shift, power spread, delay spread and AoA as given in [5] by:

$$g_{kl}(t,f) = \sqrt{P_{lk}} e^{2\pi i f_d cos(w_{kl})t - 2\pi i \tau_{kl} f} \tag{4.6}$$

where P_{lk} is the power spread, f_d is the maximum Doppler shift, w_{kl} is the AoA of the subpath relative to the direction of motion, τ_{kl} gives the delay spread and f is the carrier frequency.

The small-scale fading describes the rapid fluctuation of the amplitude of a radio signal over a short period of time or travel distance. It is caused by interference between two or more versions of the transmitted signal which arrive at the receiver at different times. This interference can vary widely in

amplitude and phase over time.

During the simulation execution, the small-scale fading is calculated at every slot (this means each 125 μs). In a different manner, for the large-scale fading, the spatial signature matrices are periodically updated every 100 ms, to simulate a sudden change of the channel.

Beamforming

As already mentioned before, multiple antenna elements with BF are essential to provide an acceptable range of communication in mmW system.

In order to support phased-array antennas, a new *AntennaArrayModel* class is developed, which contains a complex beamforming vector. For both transmitter and receiver, based on the positions and number of antennas, the beamforming vectors are extracted from a pre-generated log-file [16].

After the computation of the vectors, the BF gain from transmitter i to receiver j is given by:

$$G(t,f)_{ij} = |\mathbf{w}^*_{rx_{ij}} \mathbf{H}(t,f)_{ij} \mathbf{w}_{tx_{ij}}|^2 \tag{4.7}$$

where $\mathbf{H}(t,f)_{ij}$ is the channel matrix of the ij^{th} link, $\mathbf{w}_{tx_{ij}}$ is the BF vector of transmitter i, when transmitting to receiver j and $\mathbf{w}_{rx_{ij}}$ is the BF vector of receiver j, when receiving from transmitter i [5].

Starting from the number of antenna elements, that are 64 for the BS and 16 for the UE, the simulator can operate a directional transmission choosing one of the 16 or 8 beams for BS and UE respectively. Then, beamforming vectors are pre-generated for each beam according with the directional angle of it. In this manner, exploiting the multiple antenna configuration, a directional beam can be established and the BF gain can be computed. The method *SetSector* of the class *AntennaArrayModel* permit to load the right BF vector, based on the right directional sector in which UE and BS communicate. Giving the number of antennas in the system and the desired sector, the method returns the BF vector, of a certain width, to be employed in Equation (4.7).

There are three different types of beamforming: analog, digital and hy-

brid [8], [32].

- *Analog* BF shapes the output beam with only one radio frequency (RF) chain, using phase shifters. This model saves power by using only a single A/D or D/A, but has a small flexibility since the BS can only beamform in one direction at a time.

- *Digital* BF provides the highest flexibility in shaping the transmitted beam(s), however it requires one RF chain per antenna element. This increases the cost and complexity, but permits to transmit on multiple directions simultaneously.

- *Hybrid* (two-stage digital and analog BF procedure) BF allows the use of a very large number of antennas with a limited number of RF chains.

In the current version of the mmW ns-3 framework, only analog beamforming can be implemented.

Beam specifics In the ns-3 framework, beamforming is implemented with Uniform Linear Array (ULA). Arrays can be comprised of 8×8, 4×4 or 2×2 elements and the spacing between them is set at $\lambda/2$, where λ is the wavelength. BSs are equipped with a maximum of 64 (8×8) antennas while UEs only have 16 (4×4).

antenna configuration	# of sectors	width in degrees
64 (8×8)	16	22.5
16 (4×4)	8	45
4 (2×2)	4	90

Table 4.3: Relation between number of antennas and sectors.

It's important to highlight that there exist a correlation between beamwidth, number of antenna elements and BF gain. In particular, the more antenna elements in the system, the narrower the beams with higher BF gain. Moreover, it should be noticed that ALU antenna patterns present

some undesired lobes that must taken into account for interference purposes, when steering a beam towards a specific direction.

Interference

Although being presumably less threatening in the mmW regime, because of the directionality of transmissions, interference computation is still quite relevant in terms of system level simulations. In fact, there might be some special spatial cases where interference is non negligible. Therefore, this module proposes an interference computation scheme that takes into account the beamforming directions associated with each link.

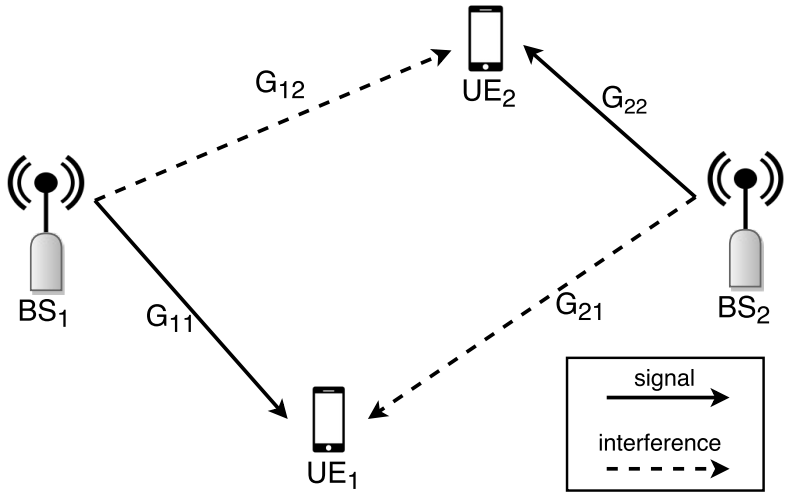

Fig. 4.5: Example of interference model.

Using Figure 4.5 as a reference, the SINR between BS_1 and UE_1 is computed as follows, first it is necessary to obtain the channel gains associated with both the desired and the interfering signals. Following Equation (4.7), we get:

$$\begin{aligned} G(t,f)_{11} &= |\mathbf{w}^*_{rx_{11}}\mathbf{H}(t,f)_{11}\mathbf{w}_{tx_{11}}|^2, \\ G(t,f)_{21} &= |\mathbf{w}^*_{rx_{11}}\mathbf{H}(t,f)_{21}\mathbf{w}_{tx_{22}}|^2. \end{aligned} \tag{4.8}$$

Then we can compute the SINR, considering also the interference as follows:

$$SINR_{11} = \frac{\frac{P_{Tx,11}}{PL_{11}} G_{11}}{\frac{P_{Tx,22}}{PL_{21}} G_{21} + BW \times N_0} \tag{4.9}$$

where $P_{Tx,11}$ is the transmit power of BS_1, PL_{11} is the pathloss between BS_1 and UE_1, and $BW \times N_0$ is the thermal noise.

4.2.3 MAC layer

The mmW modules provide also the MAC layer, that is developed using the class *mmWaveMac* which is the base class for the *mmWaveEnbMac* for the eNodeB and the *mmWaveUeMac* for the user.

The chief function of this layer is to deliver data packets coming from the upper layers to the physical layer and vice-versa. In fact this layer is designed for the synchronous delivery of upper layer data packets to the PHY layer which is key for proper data transfer in TDD mode.

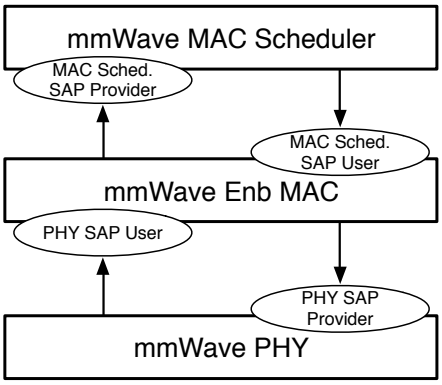

Fig. 4.6: PHY, MAC and scheduler modules with the associated SAPs.

The interfaces between the PHY and the MAC and the MAC and the scheduler are defined as Service Access Points (SAPs), as given in [33]. The relationship between modules connected through SAPs can be viewed as that of service providers and users. Figure 4.6 represents the modules with associated SAPs. The SAP provider caters to the requirement of the SAP user based on certain requests received from the user.

The eNodeB MAC layer is connected to the scheduler module using the MAC-SCHED SAP. Thus the MAC layer communicates the scheduling and the resource allocation decision to the PHY layer.

Adaptive Modulation and Coding (AMC)

The working of the AMC is similar to that for LTE. The user measures the CQI for each downlink data slot it is allocated. The CQI information is then forwarded to the eNodeB using the *mmWaveCqiReport* control message. The eNodeB scheduler uses this information to compute the most suitable modulation and coding scheme for the communication link.

The AMC is implemented by the eNodeB MAC schedulers. During resource allocation, for the current framework, the wide band CQI is used to generate the Modulation and Coding Scheme (MCS) to be used and TB size that can be transmitted over the physical layer.

Scheduler

Following the design strategy for the ns-3 LTE module [29], the virtual class *mmWaveMacScheduler* defines the interface for the implementation of MAC scheduling techniques.

The scheduler hosts the AMC module and performs the scheduling and resource allocation for a subframe with both DL and UL slots.

The TDD scheme enforced by the scheduler module is based on the user specified parameter *TDDControlDataPattern* given in Table 4.1. The slots specified for control are assigned alternately for DL and UL control channels. The data slots are equally divided between DL and UL slots with the first $n/2$ data slots allocated to DL data and rest to uplink, where n is the total number of data slots. This scheme minimizes the switching time between UL and DL data transmissions.

Resource Allocation

Using the *mmWavePhyMacCommon* object, the division of resources in the frequency domain can be customized as given in Table 4.1. The MAC sched-

uler currently implements a simple Round Robin (RR) algorithm to allocate DL and UL data slots to the connected users. All the frequency elements in a particular slot are assigned to the same user. The control slots are not allocated to any particular user. Any or all users can receive from and transmit to the base station in the control slots. For the case of the RR scheduler the use of the CQI is limited to the determination of the TB size to allocate for each UE.

Service Access Point (SAP)

The relationship between modules connected through SAPs can be viewed as that of service providers and users. The SAP provider caters to the requirement of the SAP user based on certain requests received from the user. As reported in Figure 4.6, we can identified two different SAPs [16], [33].

PHY-MAC The communication between the MAC and the PHY layer using the MAC-PHY SAP is through the following processes.

- The subframe indication is sent by the PHY layer to the MAC at the beginning of each slot. The subframe indication for slot 1 of a particular subframe triggers the scheduling procedure for the BS MAC. These indications are required for upper layer data delivery.

- The base station MAC maintains data queues for each of the connected UE and just one such queue is sufficient for the user device. Based on the scheduling scheme and the allocated resources, the MAC layer will send the scheduled number of packets (given by the TB size) to the PHY layer for transmission over the radio link.

- The scheduling and resource allocation decision received by the BS MAC from the scheduler is relayed to the PHY layer using the *mmWaveResourceAllocation* message. The PHY of the base station in turn transmits this message to all the connected users notifying all the attached devices about the scheduling decision.

- Based on the SINR of the received data slots, the UE PHY calculates the CQI and transmits it to the base station in the next UL control slot. The BS PHY on receiving the *mmWaveCqiReport* control message, relays it to the MAC.

MAC-SCHED The eNodeB MAC uses the service provided by the scheduler through the following processes.

- On receiving the subframe indication for slot 1 of a particular subframe, the MAC sends a *Scheduling Trigger Request* to the scheduler, which returns the scheduling and allocation decisions in the *Scheduling Configuration Indication* in response to the trigger.

- The BS MAC, on receiving the CQI information from the PHY, sends it to the scheduler. The scheduler needs this information for future scheduling decisions.

4.2.4 Simulation

The simulation of a network using mmW modules in the ns-3 environment is made through the following steps:

- The first step is the definition of the scenario, number of UEs and BSs and the corresponding position. Moreover, it is necessary to specify, for each UE, which is the cell to being attached and registered.

- Definition of other parameters like carrier frequency, transmission power, mobility model and path-loss model.

- Development of the main simulation program, written in C++, which implements the scenario with specific parameters.

- Run of the simulation

4.2.5 Results analysis

In order to study the results of the simulations, ns-3 is able to save some traces that capture the evolution of the system during the simulation.

In the production of results, we focus on TB size allocated[3] in each slot for each user. With the use of this trace, we can see the evolution of the system and how resources are assigned to each user.

Hence, at the end of the simulation, a *.txt* log-file is generated for each user with information about time and size of the allocation. Then with a simple MATLAB® script we parse the results and therefore average them in order to obtain the graphs in Section 6.3.

[3]Here we are referring to the size in *byte* of the transport block that are allocated by the MAC layer (*mmWaveRrMacScheduler* class) in a given slot.

Chapter 5

Sharing procedure

5.1 Blind method

We define the *blind* method as the default procedure implemented in the ns-3 framework.

Every time a simulation is run, all the frame structure of the code is configured as reported in Table 4.1. More precisely, DL slots are alternated with UL slots, under the control of the scheduler that performs a Round Robin allocated one entire slot (30 OFDM symbols) for user. These settings correspond to performing a Time Division Multiple Access (TDMA) with the addition of the RR scheduler in a way to serve equally all the UEs.

5.2 SPSH scenario between different mmW networks

Before entering in detail with the sharing procedure described in this thesis, we introduce here an example to understand the scenario we are interesting in.

Consider a scenario in which there are two mmW networks (as shown in Figure 5.1), one green and one yellow, that can represent two different operator BSs in the same area.

Assuming they are operating on the same channel and located in the same

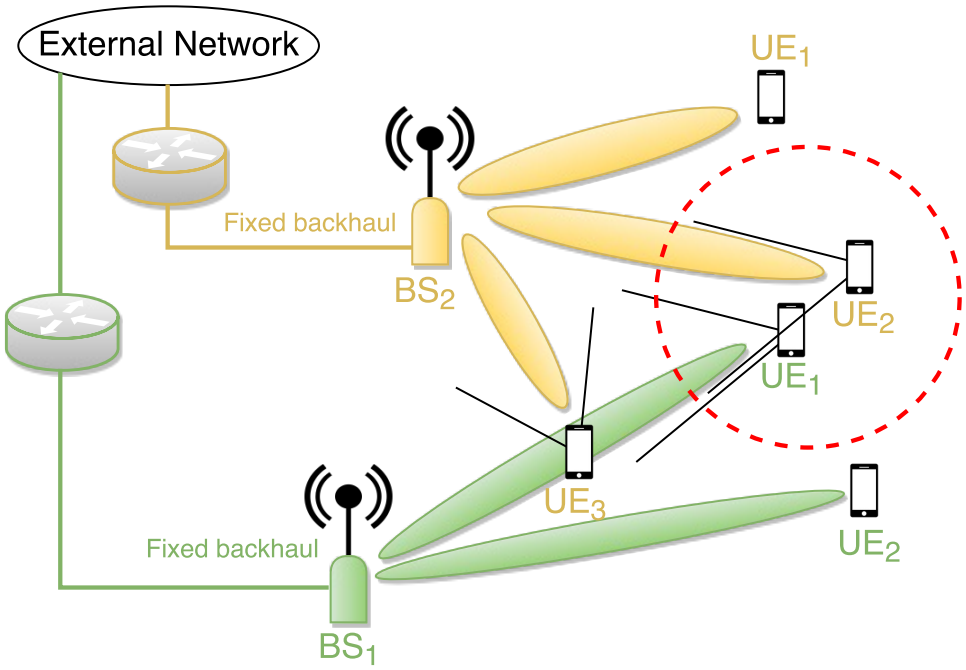

Fig. 5.1: Example of two mmW networks working in the same area.

area, depending on the directions of the beams, they might cause interference to each other.

We define the Interference Threshold (IT) as the interference level that would not trigger coordination if actual interference stays below. One example for how to define the IT is that interference up to the IT does not impact the current selection of modulation and coding at the receiver.

Other scenario assumptions are that we have a scheduled frame-based system that partitions radio resource for multiple access in the time domain, that nodes within one network are synchronized in time and frequency, and that there is at least time synchronization across networks.

The key problem to be solved in this system is how to coordinate scheduling of interfering links, between different mmW networks, so that interfering transmissions do not end up on the same radio resources and with that the non-acceptable inter-network interference is alleviated to achieve better spectrum efficiency. Hence, a coordination solution is proposed in the following to overcome the weaknesses of this reference case. The proposed solution is

similar to the one used for 4G-LTE systems, previously described in Section 3.1. The only difference is that instead of coordinating frequency resources, the coordination is in the space with directional transmission.

5.3 Training method

The objective is a solution that coordinates radio resource usage on a *per-link* basis, i.e., only transmission links that actually create non-negligible interference (beyond a given threshold IT) to particular other links should be subject to coordination. Here, coordination means that transmissions of an inter-network interference link pair (one link in one mmW network and one in the other) are subject to scheduling constraints so that they cannot be scheduled on the same radio resources (i.e., time or frequency).

The two interfering networks negotiate an agreement on such a resource partitioning and record it in the form of a Coordination Context (CC) which is stored in a Coordination Unit (CU) in each network. The CU thus represents a constraint that needs to be considered by the scheduler in each network.

For example, in Figure 5.1, green-UE_1 and yellow-UE_2 are a interfering link pair between the two different mmW networks. They will be coordinated by the CU in order to avoid interference.

Such coordination scheme can be implemented in a distributed or in a centralised way. In this thesis we will focus only on the case of centralised coordination.

5.3.1 Centralised implementation

The determination of coordination context can be implemented in a centralized way, as illustrated in Figure 5.2, where a Central Coordination Unit (CCU) is connected to multiple coordination systems, one for each network, and each of them receives coordination information from CCU.

The key idea of centralized implementation is that CCU collects the full interference information from different mmW networks and makes final de-

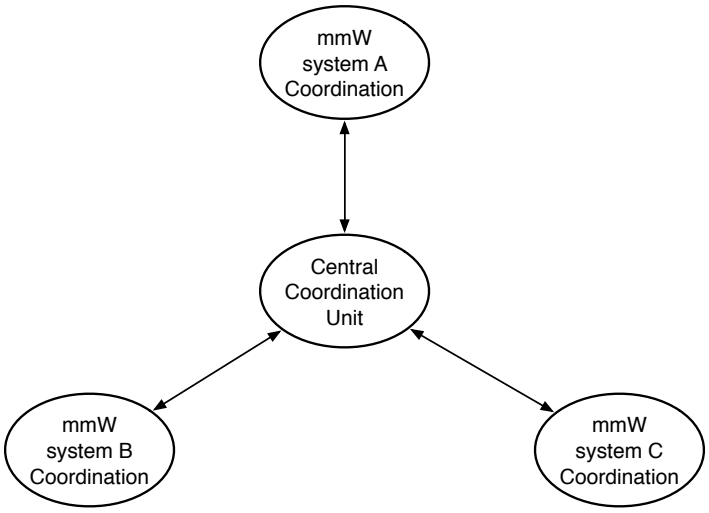

Fig. 5.2: Illustration of a centralised coordination among three different mmW networks.

cisions on the links which need CC to avoid interference above the acceptable IT.

5.3.2 Training algorithm and ns-3 implementation

In the case of centralised implementation the following procedure would be needed:

***Step 1* - Inter-network interference detection:** is operated in each BS through a measurement process already present in the LTE standard. In order to facilitate the CC concept, the interference is identified in terms of CQI level. As already mentioned in LTE, transmission of CQI messages is automatically performed by all the UEs immediately after having received a DL slot. In this manner, each BS can identify the victim UEs by reading the CQI messages received.

Knowing that, starting from the original ns-3 framework, designed by the NYU Wireless Group [16], we add a class that has the role of central control unit. The CCU has been implemented as a class called *TrainingUnit* (TU). At the beginning of each simulation, this class is initialised, and so connected

with each BSs and ready to store interference information.

***Step 2* - Interference information transfer:** The measured interference information will be transferred to the CCU in order to form the basis for the CC decision. The interference information will mainly include the Radio Network Temporary Identifier (RNTI) of the transmitter ID (unique inside the BS), the cell ID and the CQI value.

TU class, after initialization, is able to receive and save CQI values arrived from the *mmWaveEnbPhy* class. This last proceeds with the transmission of CQI information calling method *saveCqi*, only in the case the training procedure is enabled, otherwise it keeps the CQI message and uses it only to determine the allocation size of the future transmissions.

In addition to keeping all the interference information, TU coordinates also the schedule of the BS transmissions in order to receive a complete interference table for each user in the system.

***Step 3* - Coordination context decision:** Through collecting information from multiple BSs, the TU class can obtain interference information from the involved multiple connected networks. Based on this information, TU then establishes an interference graph by considering a node and an interference relationship as vertex and edge respectively. In order to avoid severe interference among different mmW networks, the interference pair of nodes (i.e., green-UE_1 and yellow-UE_2 in Figure 5.1) should be scheduled to different (i.e., orthogonal) radio resources. If we connect with an edge all the nodes that can't be allocated in the same resources the CC determination problem becomes the following graph coloring problem:

Graph coloring problem: Given a graph $G(V, E)$, where V is the set of vertices and E is the set of edges, find minimum k, and mapping $r : V\{1, ..., k\}$ such that $r(i) \neq r(j)$ for each edge $(i, j) \in E$.

In this way, the algorithm ends with the k pairs of nodes that can transmit in the same resource allocation.

Graph coloring is one of the most notorious NP-complete problems. Numerous algorithms have been developed for approximate coloring [34]. In this thesis, following [24], the simple greedy algorithm starts with some permutation of the vertices and as each vertex is considered in turn, it is assigned the minimum color that does not cause a conflict.

In the case in which the number of colors k used to solve the problem is bigger than the number of UEs per BS the algorithm ends with a sequence of nodes to be scheduled that can be the non-optimal case. Moreover, in a situation in which a UE is far from the BS or is in a condition of NLOS its CQI will be small independently from the interference of the other UEs around and, from the point of view of a graph coloring problem, that specific node can't be allocated with any other. This corresponds to the case in which the coloring algorithm ends with a non-optimal solution. From a realistic point of view, this is not a problem because, in the case in which a UE has a small value of CQI, it will not be able to communicate and report its presence in the network[1].

At the end of the procedure, a CC database is established and transmission will be scheduled with the new ordered sequence that avoids interference conditions.

All the procedures described here are made from the TU class with the help of a *Graph* object that is created immediately after having completed the interference CC database. All the interfered pairs present in the database are added as links between nodes in the graph and at the end a Greedy coloring procedure starts, calling method *greedyColoring*, providing a transmission sequence that avoids to pair interfering nodes.

***Step 4* - Scheduling:** Once the ordered sequence is determined for each BS, the CCU transmits to each of them the sequence that provides sharing of resources without interference.

In the ns-3 framework this transmit procedure is made in the other way around, each time the *mmWaveRrMacSheduler* class has to schedule a UE,

[1]This behavior is due to a limitation of the simulator that is notable to exclude UEs in outage.

if the training procedure is enabled, the method *getNextToShed* is called providing the RNTI of the next UE that has something to transmit following the sequence of the non-interfered pairs.

Figure 5.3 shows how the ns-3 framework is implemented. In particular, we refer to the methods and classes we have modified in order to make the protocol work.

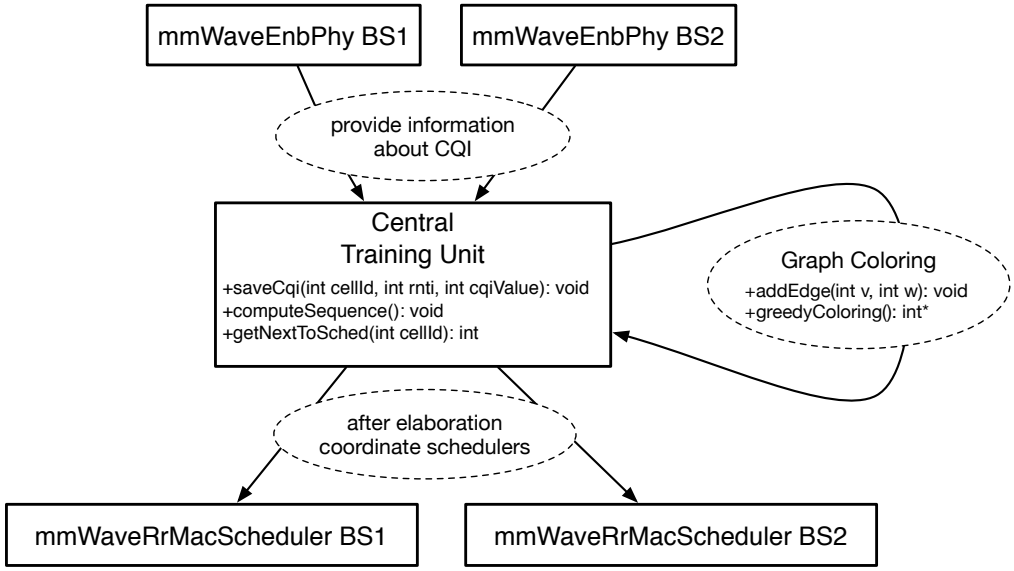

Fig. 5.3: Block diagram for the training procedure in the case of two BSs.

An important consideration in this method is related to the time necessary for the training. The CC database obtained from the initial training requires a computation time that depends on the total number of users in the system. Consider a system with m BSs and n_i UEs for BS i, then the total training time is the following:

$$t_T = \prod_{i=1}^{m} n_i \cdot 2t_{slot} + t_c \tag{5.1}$$

where t_c is the computation time required to create the CC database and share it among BSs scheduler.

Clearly this time is exponential with the number of UEs in the system. A drastic reduction of t_{slot} can provide a small t_T but, in that case, a re-design

of the frame structure of the ns-3 code is necessary.

5.4 Heuristic method

We implemented and studied also a different approach in which there isn't a training procedure that provides a complete table of interference condition and CC database, but we periodically proceed with a swap in the transmission scheduler order using the small amount of interference information exchange in each sub-frame.

5.4.1 Heuristic algorithm and ns-3 implementation

Implemented as before in a centralised way, the procedure is the following:

***Step 1* - Initialization:** Starting from a normal transmission where a Round Robin scheduler is implemented, each BS begins to receive CQI values for each DL slot allocated.

In the ns-3 framework, at the beginning of the simulation, a *ControlUnit* class is initialised and again, as the TU, is connect with each BSs.

***Step 2* - Sampling and processing:** As in the training approach, all the CQI values with attached RNTI and Cell ID are transmitted to the CCU. This procedure has been obtained with the call of the method *saveCqi* of the *ControlUnit* class.

In a different manner from before, here the CCU reads all the CQI and performs a swap in the order, only in the case the minimum CQI value is below a fixed interference threshold.

In this approach, the code provides a change in the scheduled order by processing only a part of the total interference information. Therefore, the change performed can result in a better or worse situation. In order to reduce the number of changes that result in a worse situation, the *ControlUnit* class

saves all the changes made in the past[2]. This helps the code to choose the future swaps in a way to avoid cycling repetition or previous conditions.

***Step 3* - Share of sequences:** After the procession, the CCU stores the new sequence just processed and transmits it to all the BSs. When the BSs receive the new sequence, they perform the transmission continuing to send CQI information to the CCU. After a fixed time, that depends on the computation of the data and the coordination of the schedulers, the whole procedure can be repeated starting again form *step 1*.

The *ControlUnit* class keeps trace of the order in which the transmission is computed and so can easily identify future interference conditions.

As in the training procedure, when each BS scheduler (*mmWaveRrMacScheduler*) have to allocate the transmission of a UE, it calls the method *getNextToSched* in order to receive the RNTI of the next transmitting element.

Figure 5.4 shows the class connection for the ns-3 implementation. Here, in a different way from the training procedure, the algorithm continues to run periodically until all the CQI values are above a defines threshold.

Working in a different manner than the training procedure, this heuristic method doesn't require particular computational time. The BSs can process the CQIs received without stopping the transmission by working in a parallel way.

[2]Obviously in this procedure the memory to store the changes is limited. In the execution of the results we had enough space to store all the changes in 200ms. For future implementation a study is necessary in order to provide a good trade-off between the space used for saving changes and the improvements of the algorithm.

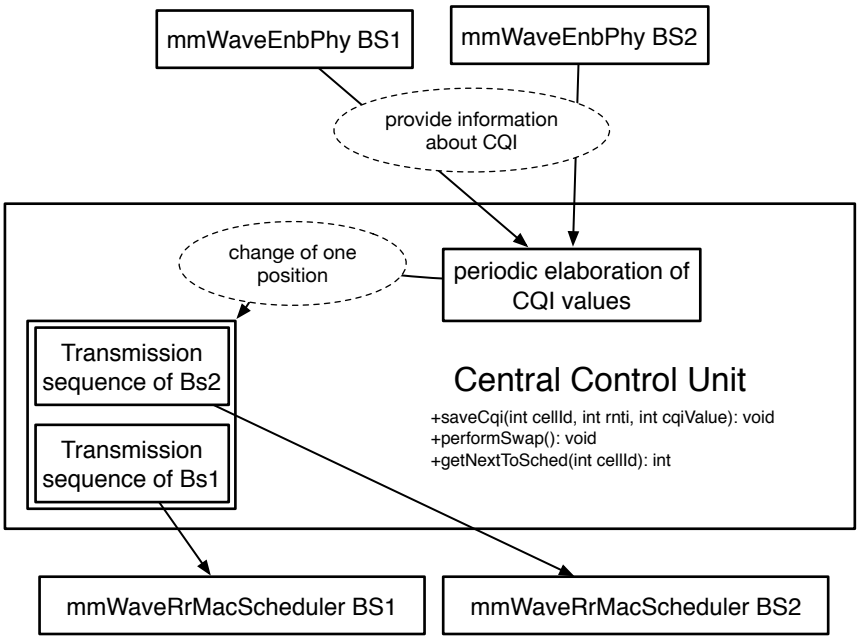

Fig. 5.4: Block diagram for the heuristic procedure in the case of two BSs.

Chapter 6

Simulated scenarios and results

6.1 Simulation assumption

In all the simulations we will present in this section, we have used the ns-3 framework just described above (Section 4.2) under the following assumptions.

We will work at the frequency of 28 GHz as carrier frequency for the mmW channel. More precisely, the total 72 sub-bands that form the 4 RB are spread between 27.5 and 28.5 GHz. In addition, we could have used the other frequency of 73 GHz that is also available in the ns-3 model, but knowing the characteristic of the propagation explained in Section 2.2.1 we analysed only the 28 GHz.

We will assume a static deployment, where users and BSs can't move during the simulation. In this way, no handover management is required, path loss and directional beam for the transmission to a specific UE doesn't change during the run of the simulation. In the future works, additional feature (like handover management, mobility, etc) must be implemented in such a way we can simulate more complicated scenarios.

We will assume to work in a dense urban environment, since the spatial statistical model provided in [5] has been realised in it. In the literature this new model is the first that includes channel parameters for mmW like path loss, number of spatial clusters, angular dispersion and outage.

We will also assume to always use analog beamforming, steering directional beams between BSs and UEs.

All these preliminary assumptions do not affect the performance of the spatial SPSH procedure here presented and studied. In the near future, when the ns-3 framework will have more sophisticated features all these assumptions will be removed or relaxed.

6.1.1 Jain's fairness index

Fairness metrics are used in network engineering to determine whether users or applications are receiving a fair share of system resources. There are several mathematical and conceptual definitions of fairness, but in this thesis we decided to use Jain's fairness index [35] to study the fairness behavior of the approaches implemented.

Raj Jain's equation:

$$\mathcal{J}(\eta_1, \eta_2, \cdots, \eta_n) = \frac{\left(\sum_{i=1}^{n} \eta_i\right)^2}{n \sum_{i=1}^{n} \eta_i^2} \tag{6.1}$$

rates the fairness of a set of values where there are n users and η_i is the throughput for the i-*th* connection. The result $\mathcal{J}$, ranges from $\frac{1}{n}$ (that represents the worst case) to 1 (best case), and it is maximum when all users receive the same allocation.

In the scenarios we are going to study, this index can help to evaluate the performance. If in a system Jain's index increases, this means that resources are better assigned among all the UE. Otherwise if the index decreases, this means we are allocating more resources for some UE instead of equally distributing them among all the UEs.

6.2 Simulated parameters

In all the simulations executed in this thesis project, we have used the parameters reported in Table 6.1. Moreover, all the specifics of the original ns-3 framework (described in Chapter 4) are kept as default in addition to the

channel model obtained from the measurements of [5].

Parameter	Value
OFDM symbols per slot	30
OFDM symbol duration	$4.16\,\mu s$
Total Bandwidth	1 GHz
Transmission power (P_{TX})	30 dBm
Noise Figure	5 dB
f_c	28 GHz
Cell radius (R)	varied in the simulation
BS antenna	8×8 ULA
UE antenna	4×4 ULA
Simulation Time	200 ms
BSs position	2 BSs both in $(0, 0, 0)$
UEs position	uniformly distributed in the cell
Propagation loss model	LoS, NLoS, outage

Table 6.1: Simulation parameters for the simulations of all the procedures.

Every time we refer to the cell radius R we mean that UEs are randomly placed, with uniform distribution, inside the cell which corresponds to a circle centered in the origin (where the two BSs are placed) and radius equal to R.

The results will be studied for the three different methods, here summarized:

- **the blind** method is the default execution of the framework where no additional computations are made in the scheduler decision.

- **the training** method starts as blind but with the training obtains a complete CC database in such a way to change the order of the transmission scheme in the scheduler.

- **the heuristic** method starts as blind but, immediately after having received the CQI values, performs swaps of positions in the transmission order scheme of the scheduler.

6.3 Description of the results

6.3.1 Different antenna configuration

The first result we analyse here is a comparison of the time evolution of the three methods in three different antenna configurations. The configurations analysed are the cases of 64−16, 64−4 and 4−4 antenna elements per BSs an UEs respectively. From Table 4.3, knowing the number of antenna elements it's possible to identify the number of sectors in which the directional transmission can be performed.

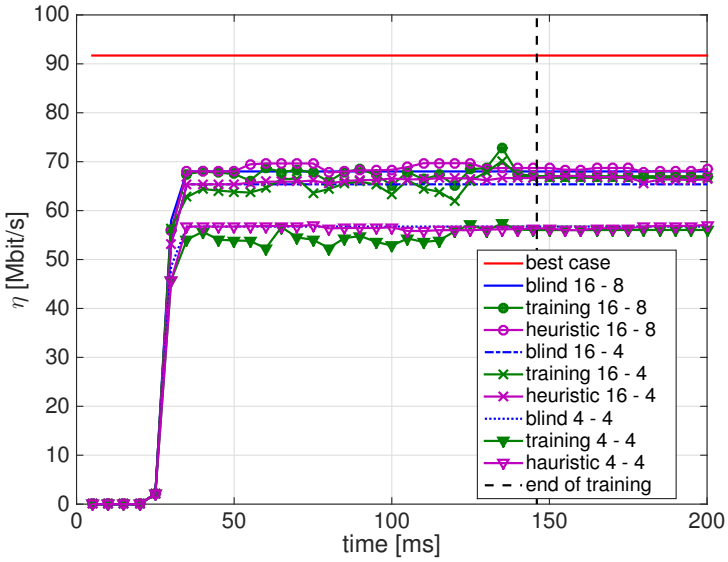

Fig. 6.1: Evolution of the three methods, for different configurations of antennas for BS and UE. Configuration with 16−8, 16−4 and 4−4 sectors for BS and UE respectively.

Figure 6.1 (zoomed view in 6.2) represents the average throughput allocated[1] η over time, where 40 UEs are randomly positioned in a cell with $R = 30$ m and the two BSs are both in the origin (0,0,0). The simulations evolve for 200 ms and, due to the complexity of the entire ns-3 simulator, each simulation required 20 minutes to be computed, for this reason, only 20

[1]Every time we mention the throughput allocated η, we refer to the TB size allocated by the scheduler at the MAC layer.

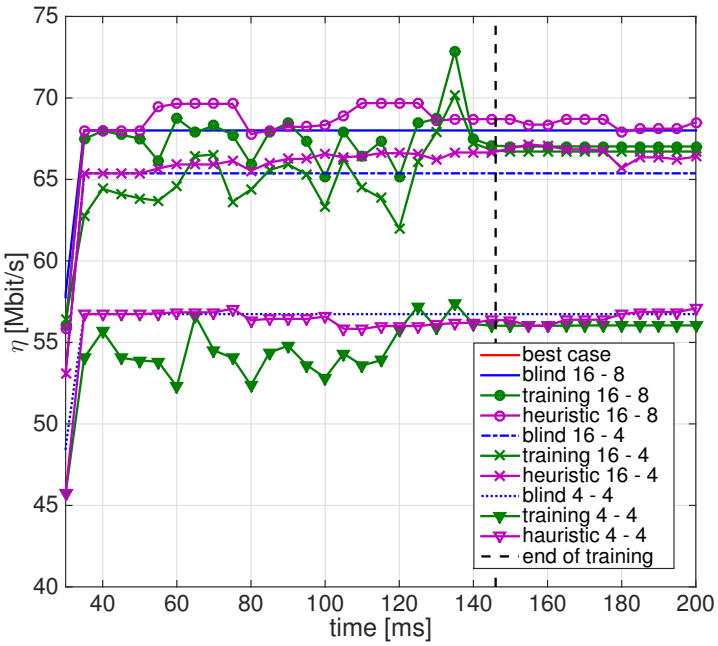

Fig. 6.2: A zoomed view of the evolution after time t_{start}, of the three methods, for different configuration of antennas for BS and UE. Configuration with 16−8, 16−4 and 4−4 sectors for BS and UE respectively.

repetitions for each cases has been made in this plot.

The best case happens when all the resources are equally distributed among all the UEs. Naturally all the UEs must have a high SINR (and so CQI) in order to use the optimum modulation scheme that permits the transmission of a TB with around 57300 bytes per slot. Therefore in this particular case, where we have 20 UEs per BS, the maximum throughput we can have is:

$$\eta_{max} = \frac{57000 \cdot 8}{20 \cdot 250\mu s} = 91.2 Mbit/s \tag{6.2}$$

The transmission starts after the initialization time that is $t_{start} = 21$ ms, then knowing the training time t_T (from Eqaution 5.1), in the simulation the training ends at:

$$t_{end} = t_{start} + t_T = t_{start} + \prod_{i=1}^{m} n_i \cdot 2t_{slot} + t_c = \tag{6.3}$$

$$t_{end} = 21ms + (20 \cdot 20)2 \cdot 125\mu s + 5 \cdot 20 \cdot 250\mu s \cong 146ms \qquad (6.4)$$

Here the computation time t_c required to create the CC database and share it among BSs is around 5 sequences of transmissions.

		$\mathcal{J}$ **fairness index**	**TB size** $[Mbit/s]$
BLIND METHOD	$16-8$	0.8055	68.01
	$16-4$	0.7842	65.37
	$4-4$	0.7088	56.74
TRAINING METHOD	$16-8$	0.7798	67.02
	$16-4$	0.7400	66.71
	$4-4$	0.7020	56.04
HEURISTIC METHOD	$16-8$	0.8236	68.51
	$16-4$	0.7981	66.39
	$4-4$	0.7105	57.09

Table 6.2: Average fairness index and throughput measured at time $t = 200$ ms, of the three methods, for different configuration of antennas for BS and UE. Configuration with 16−8, 16−4 and 4−4 sectors for BS and UE respectively.

The first thing to be noted in Figure 6.1 and Table 6.2, is that the average throughput decreases when decreasing the number of antenna elements. This is due to the BF gain of the directional beams, following Table 4.3, the higher the number of antenna elements, the smaller the width of the sector and the higher the BF gain. Therefore, the worst case in the graph corresponds to 4−4 (only 4 antenna elements per BS and UE) where the throughput is around 56.04 Mbit/s.

About the performance of the three sharing methods, the result shows that really small improvements are made. In particular, heuristic increases and decreases randomly concluding just above the blind method. Then the training method, when the coordination is finished (after 146 ms), ends with a value that sometimes is a little higher and sometimes lower than the blind.

Another consideration is that results obtained in the training method are pessimistic due to the impossibility of ns-3 simulator to exclude UEs in outage condition. This problem is currently under review, in order to find a solution.

This strange behavior may depend on several variables and factors, first of all we have that sometimes the Greedy algorithm, used for computing the CC database, can provide a non-optimal solution due to the presence of UEs which have a really small SINR independently from the presence of interference. Then, another fact is that all the results obtained have a high variance probably due to complexity of the channel model used in the framework [5]. Due to the long time necessary to simulate only one realization, it's hard to repeat a lot of times the experiment in order to reduce the variance of the estimate. All these factors, together, lead to somewhat inaccurate results.

In the next section we provide a measure of the results' variance.

Variance of the result

Another thing that results from the graph (Figures 6.1 and 6.2) is that values are really spread and the process simulated has a high variance.

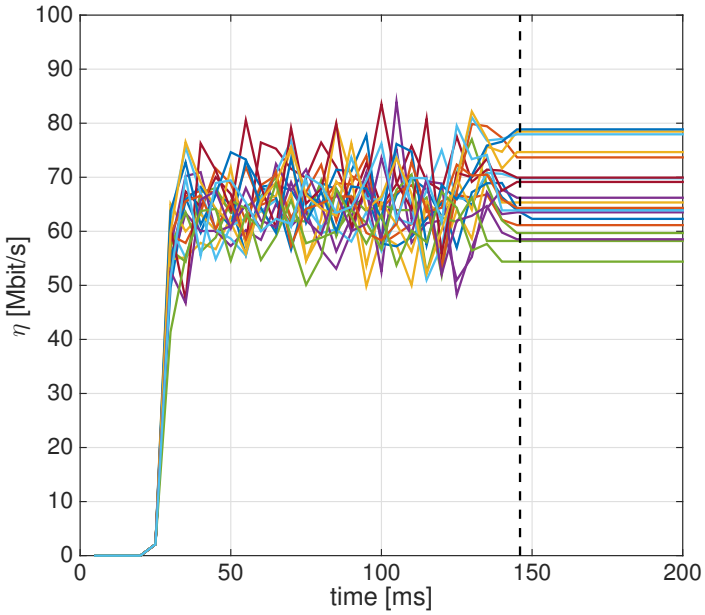

Fig. 6.3: Example of 20 different runs for the training method in the case 16−4 of Figure 6.1.

As can be seen from Figure 6.3 the variance is so high that with the same

parameters the throughput may change from 54.39 to 78.86 Mbit/s. This is due to the complexity of the entire ns-3 framework (explained in Chapter 4), so that the propagation loss model obtained from the measurements provided in [5] makes the channel matrix widely variable.

With these results, it is not possible to assure the fairness values and throughput obtained, a large number of realizations should be performed in order to have more precision in the results.

The same behavior can be seen in Figure 6.4 which is shows the mean and standard deviation for 20 different runs of the training method in the case of 16−8 antenna elements.

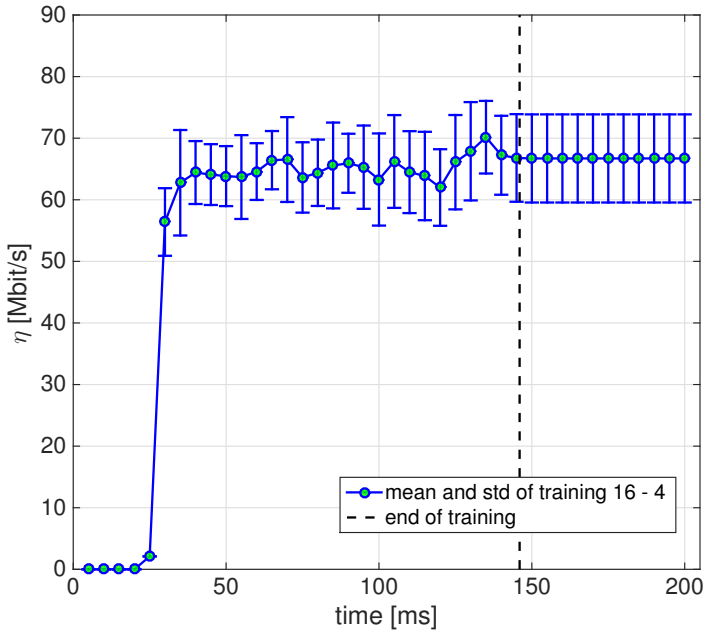

Fig. 6.4: Mean and standard deviation of the 20 different runs for the training method in the case 16−4 of Figure 6.1.

6.3.2 Other results

Future 5G cells will provide service for thousand of UEs and we would like to see the behavior of the procedures with an high number of UEs and knowing that the maximum number of UEs allowed in the ns-3 framework is 40, we

have decided to dispose the users in a specific area of the cell in order to increase the condition of interference. Moreover, we increase here the number of repetitions to 80, in order to have a more accurate measure of fairness and throughput allocated.

The area chosen corresponds to 1/4 of the entire cell so UEs can be placed with a random angle in the interval $[0, 90]$ degrees.

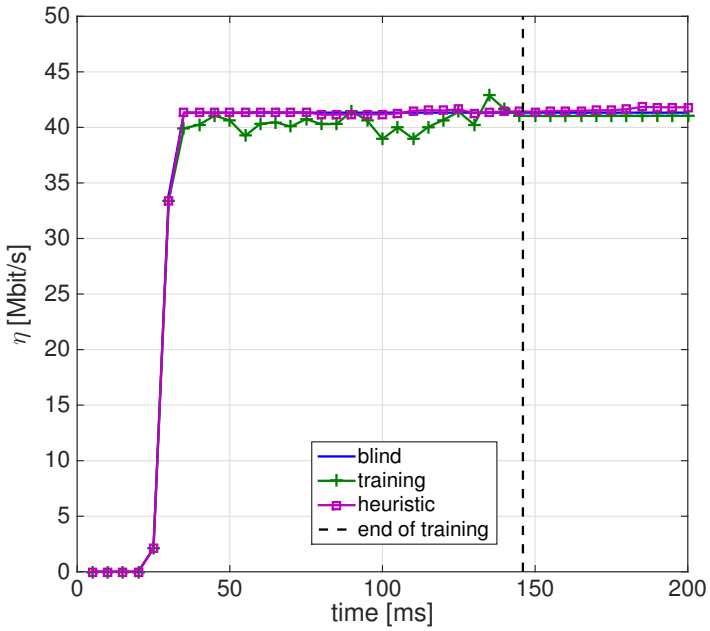

Fig. 6.5: Evolution, of the three methods, with cell radius $R = 10$ m and configuration of 16−8 sectors for BS and UE respectively.

Comparing the throughput of Figure 6.1 with that of the two Figures 6.5 and 6.7 (zoomed views in 6.6 and 6.8, respectively), we immediately notice that in the first configuration its values is higher. The small value of throughput allocated in this simulations is due to the fact that by placing the UEs only in 90 degrees of the total space only 4 sectors out of the total 16 can be chosen so when transmitting, also if we select for the two BSs the two furthest sectors, they will create a small amount of interference to each other due to the secondary lobes of ALU antennas. This interference reduces the SINR, therefore the CQI and consequently the throughput allocated.

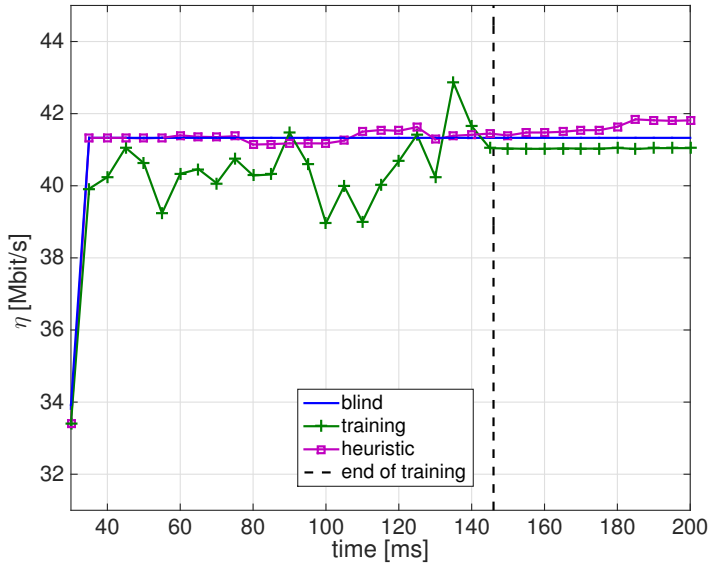

Fig. 6.6: A zoomed view of the evolution after time t_{start}, of the three methods, with cell radius $R = 10$ m and configuration of 16−8 sectors for BS and UE respectively.

Also in here with 80 runs, the differences between the two simulations with $R = 10$ m and $R = 50$ m and among the three methods are really small.

What we were expecting to see is that the blind method performs quite well, followed by the heuristic approach that brings a little improvement and, on top of this, the training approach which identifies the maximum throughout that can be reached (knowing that all the possible combinations are tried) with respect to the fairness among users. What really happens is that the variance of the results is so high that all the methods behave almost equivalent, since they evolve into the same interval. With this variance, each time a run is added the results change more than the difference between the methods. More simulations are necessary to increase the accuracy of the measure. Moreover we should analyse a more complex scenarios where the number of BSs are greater than two.

Comparing these results with the ones in the prior art, the result in [24] shows high improvements by performing training, with respect to the blind method. Improvements can find an explanation in the use of directional

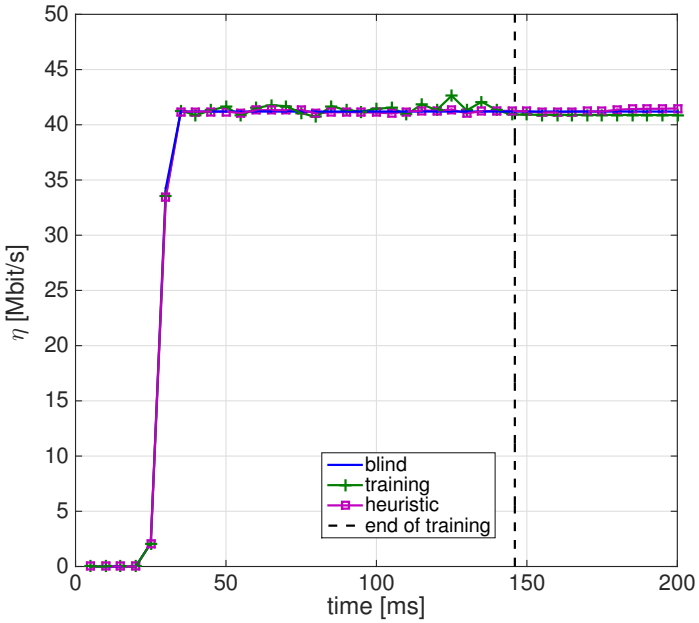

Fig. 6.7: Evolution, of the three methods, with cell radius $R = 50$ m and configuration of 16−8 sectors for BS and UE respectively.

transmission for the BS and omnidirectional transmission for mobile users. This kind of transmission results more often in interference among UEs than the case where directional transmission are used for both transmitter and receiver, thus coordination provides a better use of resources. The differences in the improvements, between the prior art and the thesis, are due to the diverse simulation conditions knowing also that in [24] UEs were placed in a small indoor area using a completely different channel model.

For this reason we can conclude that, for a system where the number of users is not very large, the blind method with fully directional transmission performs quite well.

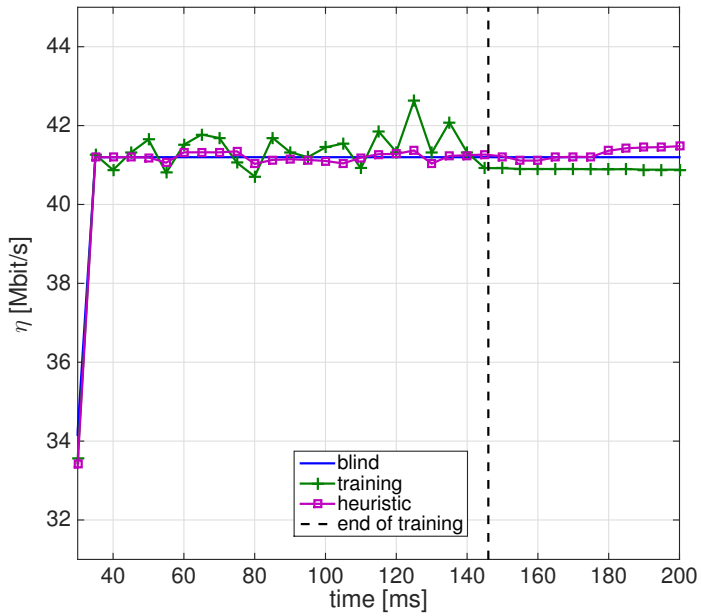

Fig. 6.8: A zoomed view of the evolution after time t_{start}, of the three methods, with cell radius $R = 50$ m and configuration of 16−8 sectors for BS and UE respectively.

		$\mathcal{J}$ **fairness index**	**TB size** $[Mbit/s]$
BLIND METHOD	$R = 10m$	0.6312	41.33
	$R = 50m$	0.5699	41.20
TRAINING METHOD	$R = 10m$	0.6279	41.04
	$R = 50m$	0.5709	40.88
HEURISTIC METHOD	$R = 10m$	0.6383	41.81
	$R = 50m$	0.5711	41.48

Table 6.3: Average fairness index and throughput measured at time $t = 200$ ms, of the three methods, for different configuration in the position of UEs. Configuration with $R = 10$ m and $R = 50$ m.

Chapter 7

Conclusions and future works

In this thesis, we studied and implemented a training procedure that should provide coordination context in a way to increase performance. We also introduced a heuristic approach that aims as well to increase the performance, working simultaneously with the transmission and so the evolution of the systems.

Staring from sharing procedures already implemented in WLAN and LTE standards, we have studied similar procedures able to work at mmW frequencies.

Then with the use of the discrete simulator ns-3 we implemented and aggregated specific class modules that permit the simulation of the algorithms studied in the thesis.

The starting idea was to develop and so measure the improvements the training should have provided, as in the prior art [24], in order to have an upper bound, with respect to fairness among users, that is the maximum achievable. The results obtained show that the process has a high variance that is due to the impossibility to compute a very large number of realizations and to the complexity of the mmW channel model used in the ns-3 simulator. For this reason we can't see and measure any kind of significant improvement.

Despite the somewhat negative results obtained in this thesis, this is the first step that has been made to study the performance of a coordination

context-based spectrum sharing where directional transmission is perform in a mmW channel.

More and more studies are necessary, starting from this first result, in order to design a protocol that uses, in the best way, the resources for a future mmW 5G system. A lot of challenges are to be faced, and for this reason, a system where directional transmissions are coordinated with frequency or time resources are necessary.

A collaboration has started with the Wireless Group at NYU in order to improve the ns-3 framework designed by them and study new protocols able to operate in situations where the number of users is really high and the blind method can't perform well.

Bibliography

[1] The 5G Infrastructure Public Private Partnership. (2015) 5G vision. https://5g-ppp.eu/our-vision/. Accessed: 2015-08-03.

[2] Ericsson, "5G radio access," February 2015, white Paper Uen 284 23-3204 Rev B.

[3] T. Rappaport, J. Murdock, and F. Gutierrez, "State of the art in 60-GHz integrated circuits and systems for wireless communications," *Proceedings of the IEEE*, vol. 99, no. 8, pp. 1390–1436, Aug 2011.

[4] M. Marcus and B. Pattan, "Millimeter wave propagation; spectrum management implications," *Microwave Magazine, IEEE*, vol. 6, no. 2, pp. 54–62, June 2005.

[5] M. R. Akdeniz, Y. Liu, S.Sun, S.Rangan, T. S. Rappaport, and E. Erkip, "Millimeter wave channel modeling and cellular capacity evaluation," *CoRR*, vol. abs/1312.4921, 2013. [Online]. Available: http://arxiv.org/abs/1312.4921

[6] P. Kyosti and et al., "WINNER II channel model," *Technical Report IST-WINNER D1.1.2 ver 1.1*, September 2007.

[7] "NGMN 5G white paper," Feb 2015, https://www.ngmn.org/home.html. Accessed: 2015-08-03.

[8] H. Shokri-Ghadikolaei, C. Fischione, G. Fodor, P. Popovski, and M. Zorzi, "Millimeter wave cellular networks: A MAC

layer perspective," *Communications, IEEE Transactions on*, 2015, 10.1109/TCOMM.2015.2456093.

[9] T. Rappaport, S. Sun, R. Mayzus, H. Zhao, Y. Azar, K. Wang, G. Wong, J. Schulz, M. Samimi, and F. Gutierrez, "Millimeter wave mobile communications for 5G cellular: It will work!" *Access, IEEE*, vol. 1, pp. 335–349, 2013.

[10] B. Bangerter, S. Talwar, R. Arefi, and K. Stewart, "Networks and devices for the 5G era," *Communications Magazine, IEEE*, vol. 52, no. 2, pp. 90–96, February 2014.

[11] T. Rappaport, R. Heath, R. Daniels, and J. Murdock, *Millimeter Wave Wireless Communications*, ser. Communication engineering and emerging technologies. Prentice Hall, 2014. [Online]. Available: https://books.google.it/books?id=_Tt_BAAAQBAJ

[12] F. Vook, A. Ghosh, and T. Thomas, "MIMO and beamforming solutions for 5G technology," in *Microwave Symposium (IMS), 2014 IEEE MTT-S International*, June 2014, pp. 1–4.

[13] L. Badia, R. Del Re, F. Guidolin, A. Orsino, and M. Zorzi, "A tunable framework for performance evaluation of spectrum sharing in LTE networks," in *World of Wireless, Mobile and Multimedia Networks (WoWMoM), 2013 IEEE 14th International Symposium and Workshops on a*, June 2013, pp. 1–3.

[14] L. Anchora, M. Mezzavilla, L. Badia, and M. Zorzi, "Simulation models for the performance evaluation of spectrum sharing techniques in OFDMA networks," in *Proceedings of the 14th ACM International Conference on Modeling, Analysis and Simulation of Wireless and Mobile Systems*, ser. MSWiM '11. New York, NY, USA: ACM, 2011, pp. 249–256. [Online]. Available: http://doi.acm.org/10.1145/2068897.2068941

[15] What is ns-3. https://www.nsnam.org/overview/what-is-ns-3/. Accessed: 2015-08-03.

[16] M. Mezzavilla, S. Dutta, M. Zhang, M. R. Akdeniz, and S. Rangan, "5G mmwave module for ns-3 network simulator," *CoRR*, vol. abs/1506.08801, 2015. [Online]. Available: http://arxiv.org/abs/1506.08801

[17] S. Rangan, T. S. Rappaport, and E. Erkip, "Millimeter wave cellular wireless networks: Potentials and challenges," *CoRR*, vol. abs/1401.2560, 2014. [Online]. Available: http://arxiv.org/abs/1401.2560

[18] S. Rajagopal, S. Abu-Surra, Z. Pi, and F. Khan, "Antenna array design for multi-Gbps mmwave mobile broadband communication," in *Global Telecommunications Conference (GLOBECOM 2011), 2011 IEEE*, Dec 2011, pp. 1–6.

[19] E. Larsson, O. Edfors, F. Tufvesson, and T. Marzetta, "Massive MIMO for next generation wireless systems," *Communications Magazine, IEEE*, vol. 52, no. 2, pp. 186–195, February 2014.

[20] L. Lu, G. Li, A. Swindlehurst, A. Ashikhmin, and R. Zhang, "An overview of massive MIMO: Benefits and challenges," *Selected Topics in Signal Processing, IEEE Journal of*, vol. 8, no. 5, pp. 742–758, Oct 2014.

[21] B. Van Veen and K. Buckley, "Beamforming: a versatile approach to spatial filtering," *ASSP Magazine, IEEE*, vol. 5, no. 2, pp. 4–24, April 1988.

[22] L. Anchora, M. Mezzavilla, L. Badia, and M. f, "A performance evaluation tool for spectrum sharing in multi-operator LTE networks," *Computer Communications*, vol. 35, no. 18, pp. 2218 – 2226, 2012. [Online]. Available: http://www.sciencedirect.com/science/article/pii/S0140366412002678

[23] W. Feng, Y. Li, D. Jin, and L. Zeng, "Inter-network spatial sharing with interference mitigation based on IEEE 802.11ad WLAN system," in *Globecom Workshops (GC Wkshps), 2014*, Dec 2014, pp. 752–758.

[24] G. Li, T. Irnich, and C. Shi, "Coordination context-based spectrum sharing for 5G millimeter-wave networks," in *Cognitive Radio Oriented Wireless Networks and Communications (CROWNCOM), 2014 9th International Conference on*, June 2014, pp. 32–38.

[25] R. Cai, Q. Chen, X. Peng, and D. Liu, "Spatial sharing algorithm in mmwave WPANs with interference sense beamforming mechanism," in *Military Communications Conference, MILCOM 2013 - 2013 IEEE*, Nov 2013, pp. 163–168.

[26] Q. Chen, X. Peng, J. Yang, and F. Chin, "Spatial reuse strategy in mmwave WPANs with directional antennas," in *Global Communications Conference (GLOBECOM), 2012 IEEE*, Dec 2012, pp. 5392–5397.

[27] J. Luo, J. Eichinger, Z. Zhao, and E. Schulz, "Multi-carrier waveform based flexible inter-operator spectrum sharing for 5G systems," in *Dynamic Spectrum Access Networks (DYSPAN), 2014 IEEE International Symposium on*, April 2014, pp. 449–457.

[28] NYU wireless. Available at: http://nyuwireless.com.

[29] G. Piro, N. Baldo, and M. Miozzo, "An LTE module for the ns-3 network simulator," in *Proceedings of the 4th International ICST Conference on Simulation Tools and Techniques*, ser. SIMUTools '11. ICST, Brussels, Belgium, Belgium: ICST (Institute for Computer Sciences, Social-Informatics and Telecommunications Engineering), 2011, pp. 415–422. [Online]. Available: http://dl.acm.org/citation.cfm?id=2151054.2151129

[30] E. Dahlman, S. Parkvall, J. Skold, and P. Beming., *3G Evolution HSPA and LTE for Mobile Broadband.* Academic Press., 2008.

[31] C. Jeong, J. Park, and H. Yu, "Random access in millimeter-wave beamforming cellular networks: issues and approaches," *Communications Magazine, IEEE*, vol. 53, no. 1, pp. 180–185, January 2015.

[32] S. Sun, T. Rappaport, R. Heath, A. Nix, and S. Rangan, "MIMO for millimeter-wave wireless communications: beamforming, spatial multiplexing, or both?" *Communications Magazine, IEEE*, vol. 52, no. 12, pp. 110–121, December 2014.

[33] FemtoForum, "LTE MAC scheduler interface specification v1.11," Oct. 2010.

[34] A. Lim, Y. Zhu, Q. Lou, and B. Rodrigues, "Heuristic methods for graph coloring problems," in *Proceedings of the 2005 ACM Symposium on Applied Computing*, ser. SAC '05. New York, NY, USA: ACM, 2005, pp. 933–939. [Online]. Available: http://doi.acm.org/10.1145/1066677.1066892

[35] R. Jain, D. Chiu, and W. Hawe, "A quantitative measure of fairness and discrimination for resource allocation in shared computer systems," *CoRR*, vol. cs.NI/9809099, 1998. [Online]. Available: http://arxiv.org/abs/cs.NI/9809099

Acknowledgements

Firstly, I would like to express my sincere gratitude to my advisor prof. Michele Zorzi for his help and his support.

A huge thank you goes to the guys of the NYU Wireless: Russell Ford, Menglei Zhang, Sourjya Dutta and Marco Mezzavilla, who wrote me hundreds of emails to help make everything work.

Another thank you to the guys of the Signet group, who I thanks for all the advices and teachings on programming.

Finally, a big hug to all the university friends who believed in me and supported me during this years. Probably, without their help I couldn't have reached this milestone.